



RETURNING MATERIALS:

Place in book drop to
remove this checkout from
your record. FINES will
be charged if book is
returned after the date
stamped below.

--	--	--

**RELATIVE SENSITIVITY OF A FAMILY OF
CLOSEST-POINT GRAPHS IN VISION APPLICATIONS**

By

Terrence L. Chorzempa

A THESIS

Submitted to
Michigan State University
in partial fulfillment of the requirements
for the degree of

MASTER OF SCIENCE

Department of Computer Science

1988

ABSTRACT

RELATIVE SENSITIVITY OF A FAMILY OF CLOSEST-POINT GRAPHS IN VISION APPLICATIONS

By

Terrence L. Chorzempa

Detecting structure in images is one of the important tasks performed early in a vision system. A common technique for structure detection involves graphs and the neighborhoods they create. The goals of this work are twofold. One is to measure the sensitivity of the Delaunay Triangulation, the Gabriel Graph, the Relative Neighborhood Graph and the Minimum Spanning Tree in locating dotted structures embedded in a uniformly distributed random dot pattern. The second goal is to measure the effect of dot position perturbations on each graph's structure.

Structure detection experiments are performed where linear structures with varying degrees of spacing, longitudinal and transverse variation are placed in a noisy background and then detected using the Hough transform. Global structures detected by the Hough transform are then refined using the neighborhood information provided by the graphs. Graph performance is measured by the amount of structure fragmentation resulting from the interference caused by the background points.

Terrence L. Chorzempa

Graph stability experiments are performed where one dot of a uniformly distributed random dot pattern is subjected to random direction perturbations. Graph performance is measured by the highest order neighbor whose vertex adjacencies have been effected.

Results indicate that the Delaunay triangulation is the least sensitive to background interference and dot perturbations.

Acknowledgements

I would like to thank my advisor, Dr. Mihran Tuceryan, for all his valuable assistance in preparing this thesis.

I also wish to thank my parents, Vincent and Mary, for their unending support and patience.

Table of Contents

List of Tables.....	vii
List of Figures.....	viii
Chapter 1 Introduction.....	1
1.1 Motivation.....	1
1.2 Thesis Problem Statement.....	19
1.3 Thesis Outline	20
Chapter 2 Structure Detection.....	21
2.1 Background	21
Chapter 3 Methodology	24
3.1 Problem to Study.....	24
3.2 Procedure.....	29
3.2.1 Generation of Structure Detection Images.....	29
3.2.2 Detection of Global Structure	33
3.2.3 Localizing the Structure using Graphs.....	37
3.2.4 Generation of Graph Stability Images.....	37
3.2.5 Identification of Altered Neighbors	38
3.3 Measures of Sensitivity	40
3.4 Experiments.....	41

Chapter 4 Results and Discussion.....	45
4.1 Experiment 1 - Spacing (20)	45
4.2 Experiment 2 - Spacing, Transverse (20).....	55
4.3 Experiment 3 - Spacing, Longitudinal, Transverse (20) ..	59
4.4 Experiment 4 - Spacing, Longitudinal, Transverse (16) ..	63
4.5 Experiment 5 - Perturbation (20)	67
4.6 Experiment 6 - Perturbation (16)	70
 Chapter 5 Conclusions	 73
5.1 Summary and Conclusions.....	73
5.2 Future Work	75
 Bibliography	 77

List of Tables

Table 4-1	Experiment 5, Significance of the Average Neighbor Orders	69
Table 4-2	Experiment 6, Significance of the Average Neighbor Orders	72

List of Figures

Figure 1-1 A Dotted Line	3
Figure 1-2 A Dotted Line Surrounded by Noise	4
Figure 1-3 A Random Dot Pattern	7
Figure 1-4 Voronoi Tessellation for Figure 1-3	8
Figure 1-5 Delaunay Triangulation for Figure 1-3.....	9
Figure 1-6 GG Circles of Influence.....	11
Figure 1-7 RNG Lunes of Influence.....	12
Figure 1-8 Gabriel Graph for Figure 1-3.....	13
Figure 1-9 Relative Neighborhood Graph for Figure 1-3	14
Figure 1-10 Minimum Spanning Tree for Figure 1-3	16
Figure 3-1 MST of a Dotted Line.....	26
Figure 3-2 MST of a Dotted Line Surrounded by Noise.....	27
Figure 3-3 Spacing, Longitudinal and Transverse Variations	32
Figure 3-4 Hough Parameters of a Line	35
Figure 3-5 Points of a Hough Detected Line.....	36
Figure 3-6 First, Second and Third Order DT Neighbors	39
Figure 4-1 Experiment 1, Small Dotted Line Perturbations.....	48
Figure 4-2 Experiment 1, Average Figure Significance Results	49
Figure 4-3 Experiment 1, MST of Small Dotted Line Perturbations ...	50
Figure 4-4 Experiment 1, DT of Small Dotted Line Perturbations	51
Figure 4-5 Experiment 1, Large Dotted Line Perturbations.....	52
Figure 4-6 Experiment 1, MST of Large Dotted Line Perturbations ...	53
Figure 4-7 Experiment 1, DT of Large Dotted Line Perturbations	54
Figure 4-8 Experiment 2, Small Dotted Line Perturbations.....	56
Figure 4-9 Experiment 2, Average Figure Significance Results	57
Figure 4-10 Experiment 2, Large Dotted Line Perturbations.....	58

Figure 4-11 Experiment 3, Small Dotted Line Perturbations.....	60
Figure 4-12 Experiment 3, Large Dotted Line Perturbations.....	61
Figure 4-13 Experiment 3, Average Figure Significance Results	62
Figure 4-14 Experiment 4, Average Figure Significance Results	64
Figure 4-15 Experiment 4, Small Dotted Line Perturbations.....	65
Figure 4-16 Experiment 4, Large Dotted Line Perturbations.....	66
Figure 4-17 Experiment 5, Average Neighbor Order Results.....	68
Figure 4-18 Experiment 6, Average Neighbor Order Results.....	71

Chapter 1

Introduction

This thesis examines the suitability of a set of related closest-point graphs in the detection of structure and explores the graph's structural stability in random dot patterns. One objective is to determine the portion of the structure retained by a particular graph when controlled amounts of distortion are introduced. The second objective is to ascertain the stability of each graph when an image point is subjected to controlled amounts of perturbation. Each one of these graphs has been shown to possess favorable characteristics as discussed in Chapter Two. In the following section, perceptual grouping is discussed. The remaining sections of Chapter One contain the thesis problem statement and goals followed by the thesis outline.

1.1 Motivation

Structural grouping using graph theoretic techniques is very prevalent [AHU 82] [FAI 83] [JAR 73] [MAT 80] [TOU 80B] [URQ 82] [ZAH 71]. There are several reasons why this is so. One reason is that there exists a large body of theoretical knowledge on graphs to draw upon. Specifically,

many efficient graph algorithms [WAR 62] [KRU 56] [PRI 57] can be used to ease the computational burden of computer vision tasks. Another reason is that graphs can be used to easily express spatial relationships between entities in an image; for example, the perception of Gestalt groupings [KOF 35] [WER 38]. The Gestalt laws of perceptual grouping are used by a vision system to organize image entities without a priori knowledge of what is contained in the image. The basis for this low level processing lies in the fact that regularity in the image plane almost always results from regularities in the physical world. The primitive structural information provided by this grouping procedure is used in more complex processes such as the perception of depth and object recognition. This view of perceptual organization allows an interpretation of vision processes in terms closely related to the characteristics of human vision. Gestalt rules include proximity, smoothness, closure and symmetry. The dots in Figure 1-1 are perceived as a line using the proximity criteria. With the addition of noise points in Figure 1-2, the line is no longer perceivable. It is the ability to capture the interactions among the image points by the graph neighbor relation that is under study in this thesis.

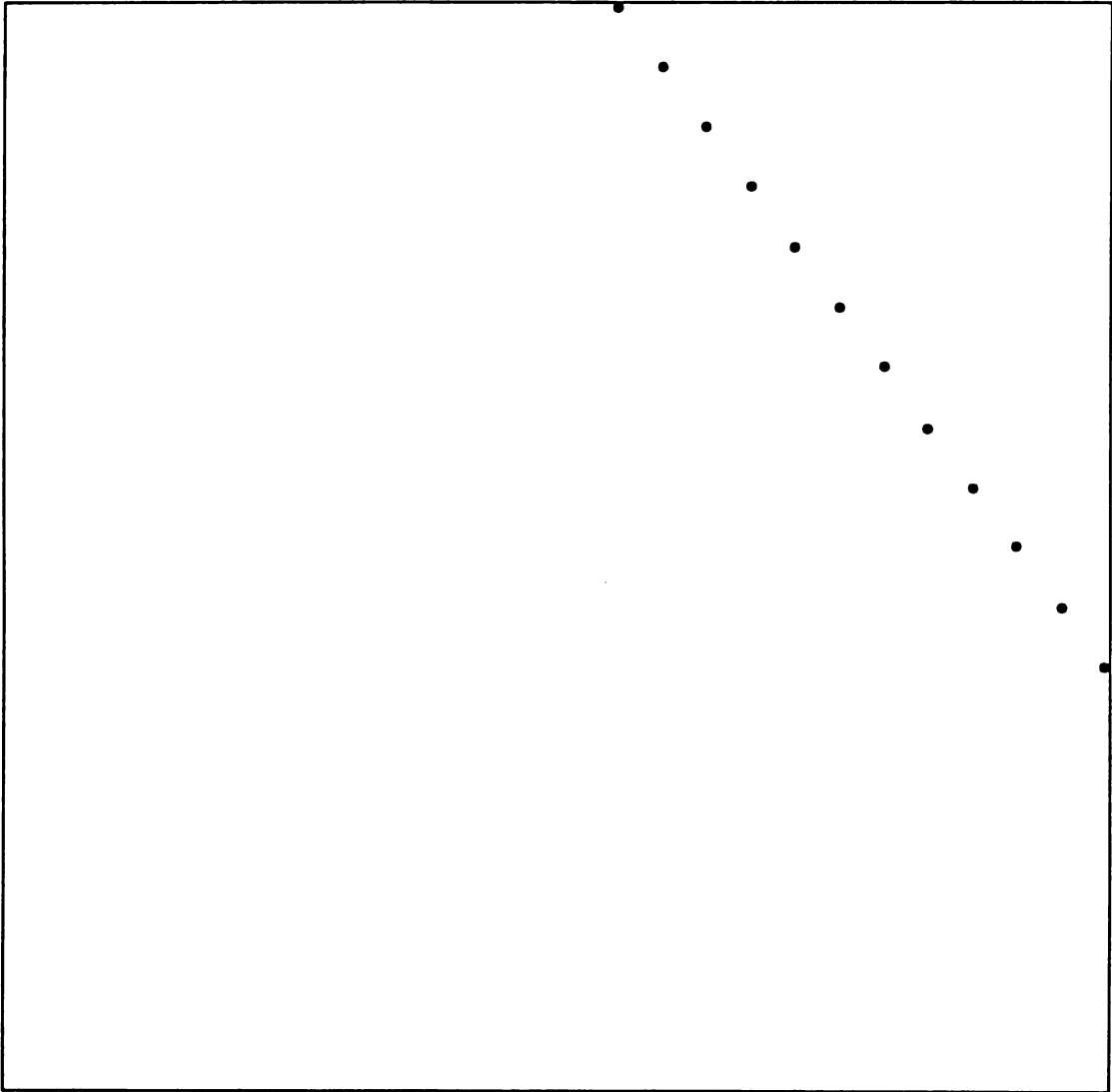


Figure 1-1 A Dotted Line

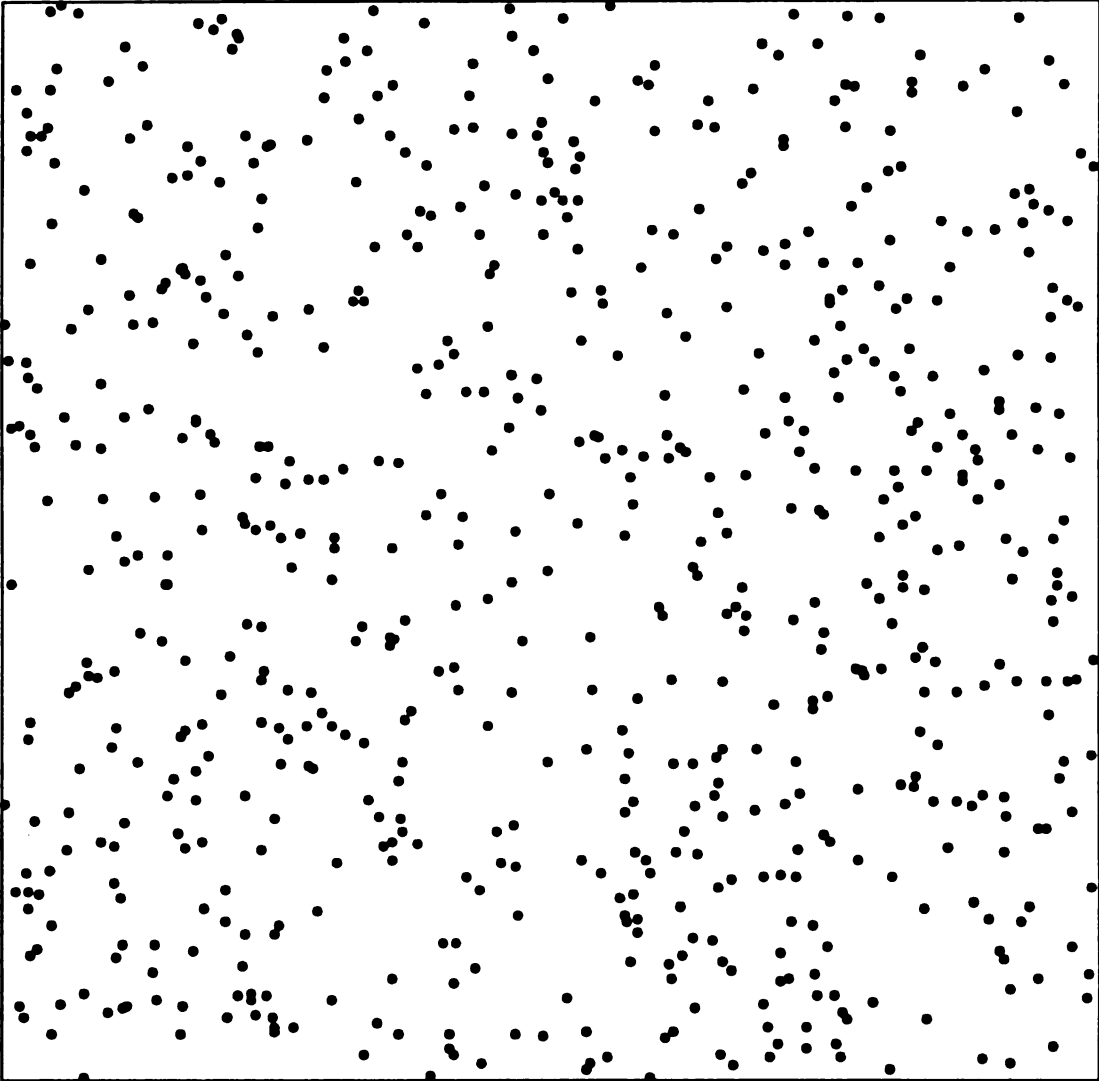


Figure 1-2 A Dotted Line Surrounded by Noise

In this thesis, the data consists of binary images. The black pixels in the image define a uniformly distributed random dot pattern. With the closest-point graphs studied here, every dot of the random dot pattern is a node (vertex) of a graph and the edges connecting the adjacent nodes are drawn based on the Euclidean distance separating the nodes. According to Gestalt rules of organization [KOF 35] [WER 38], one way the human vision system extracts structure is by grouping objects that are within close proximity to one another. In this case, the proximity criteria is expressed by the vertex adjacency relation of a particular graph and a metric on the edges.

The closest-point graphs under study in this work are the Delaunay Triangulation (DT), the Gabriel Graph (GG), the Relative Neighborhood Graph (RNG) and the Minimum Spanning Tree (MST). These graphs were chosen for evaluation because all have been suggested as valuable tools in structure identification [AHU 82] [TOU 80B] [URQ 82] [ZAH 71]. These proposals are based on the idea that each graph induces a neighbor relation on the set of image dots that can be used in applying one or more of the Gestalt laws of perceptual grouping. Another property of these graphs that contributed to their selection is that they form the hierarchy given below.

$$MST \subseteq RNG \subseteq GG \subseteq DT$$

This hierarchical relationship is important for two reasons. First, the hierarchy reflects the stringency of the graph neighbor requirements with the MST being the most stringent and the DT being the least. Secondly, with only minor modifications to the algorithm for computing the DT, any one of the other graphs can be easily obtained.

As noted earlier, the DT is a superset of all the other graphs, therefore, the GG, RNG and MST can be easily defined in terms of the DT. First of all, the DT is the dual of the Voronoi tessellation. Let S be a set of three or more points in the Euclidean plane. Assume that these points are not all collinear and that no four points are cocircular. Consider an arbitrary pair of points P and Q . The bisector of the line joining P and Q is the locus of points equidistant from both P and Q and divides the plane into two halves. The half plane H_P^Q (H_Q^P) is the locus of points closer to P (Q) than to Q (P). For any given point P , a set of such half planes is obtained for various choices of Q . The intersection $\bigcap_{Q \in S, Q \neq P} H_P^Q$ defines a convex polygonal region consisting of points closer to P than any other point. Such a region is called the Voronoi polygon [VOR 08] associated with the point P . The set of complete polygons is called the Voronoi diagram of S [SHA 75] [AHU 82]. The Voronoi diagram together with the incomplete polygons in the convex hull define a Voronoi tessellation of the entire plane. The Voronoi tessellation for the points in Figure 1-3 is shown in Figure 1-4. Two points are Voronoi neighbors if the Voronoi polygons enclosing them share a common edge. Connecting all pairs of Voronoi neighbors gives the DT. Figure 1-5 is the DT computed from Figure 1-4.

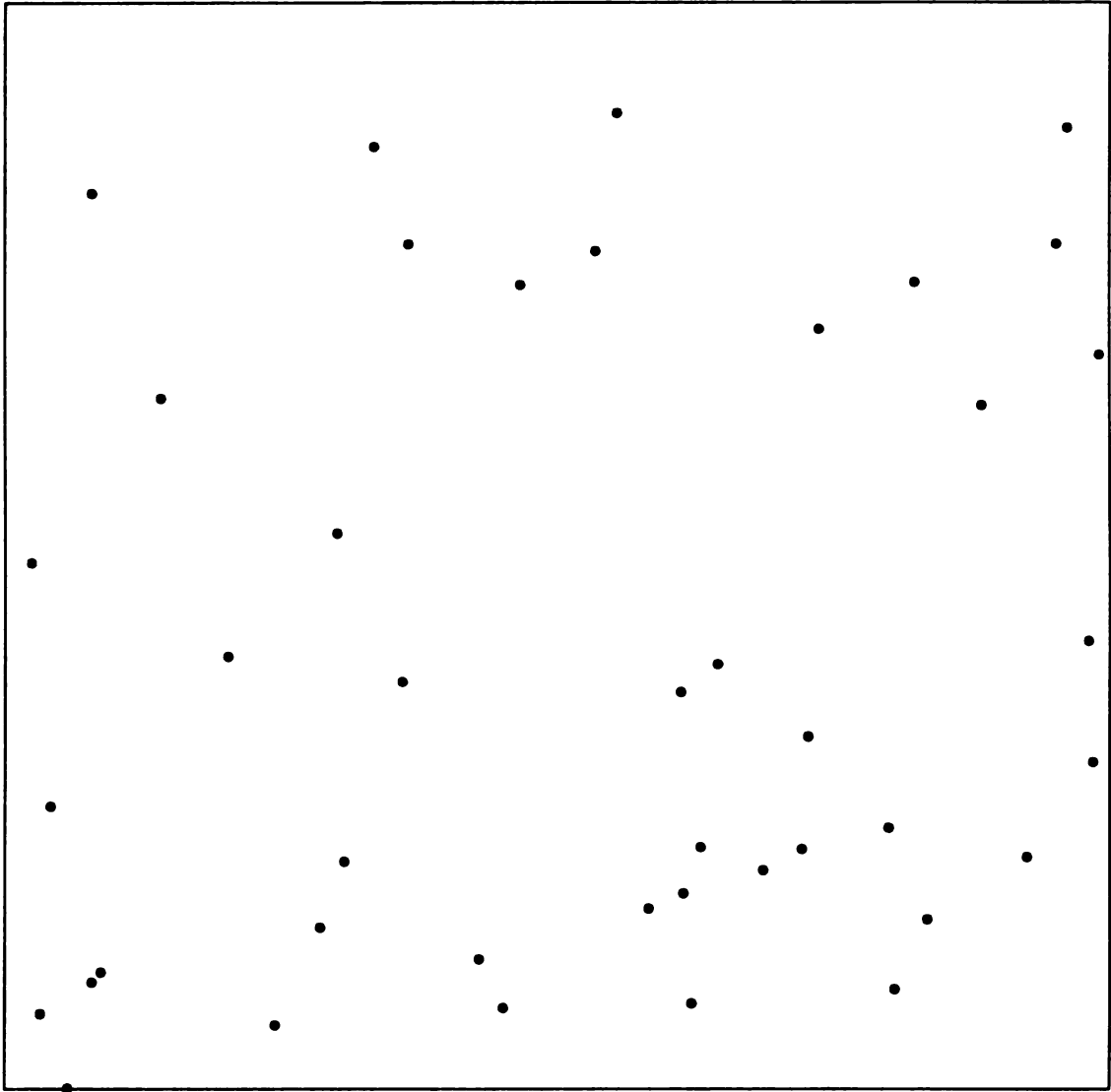


Figure 1-3 A Random Dot Pattern

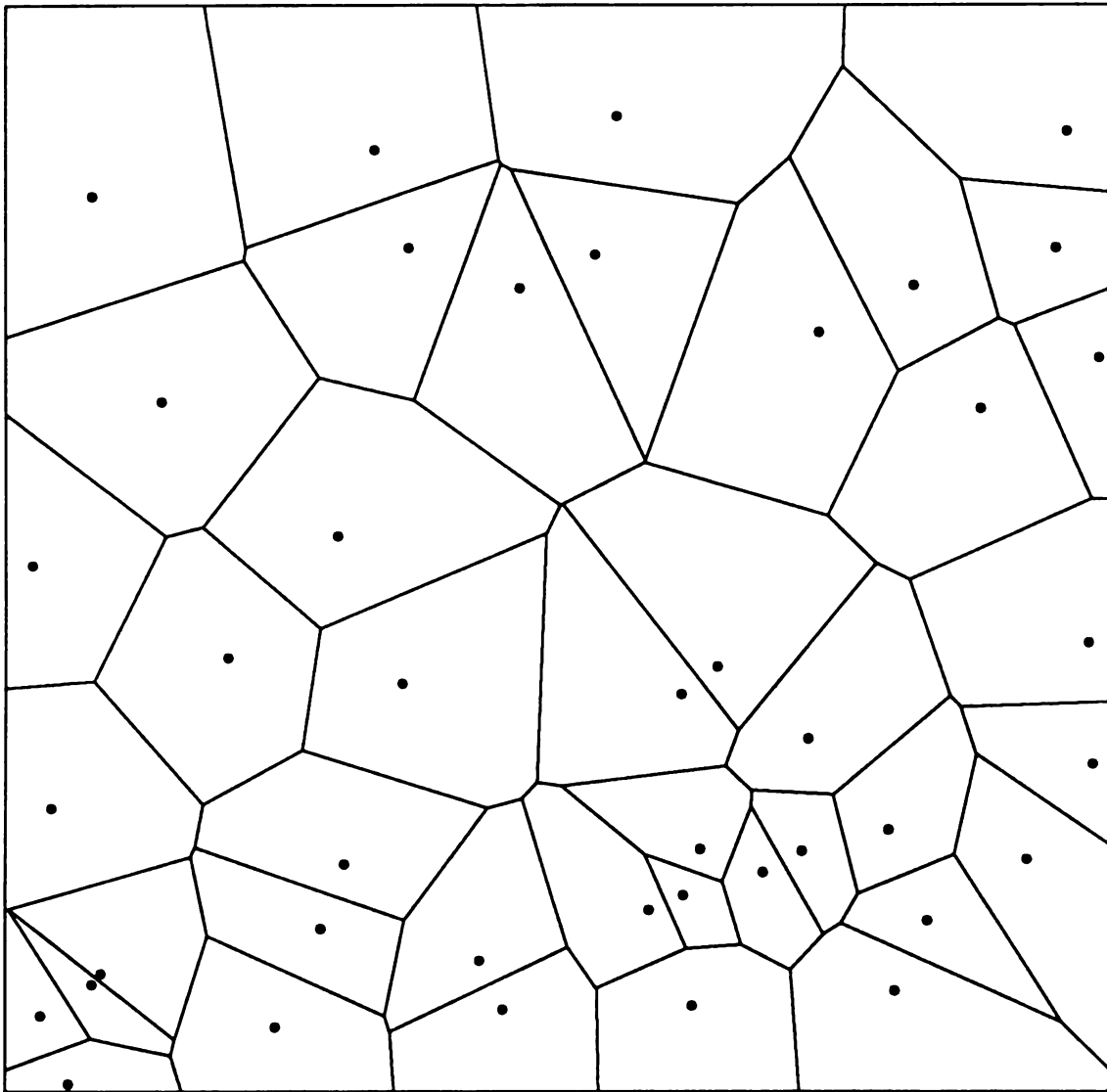


Figure 1-4 Voronoi Tessellation for Figure 1-3

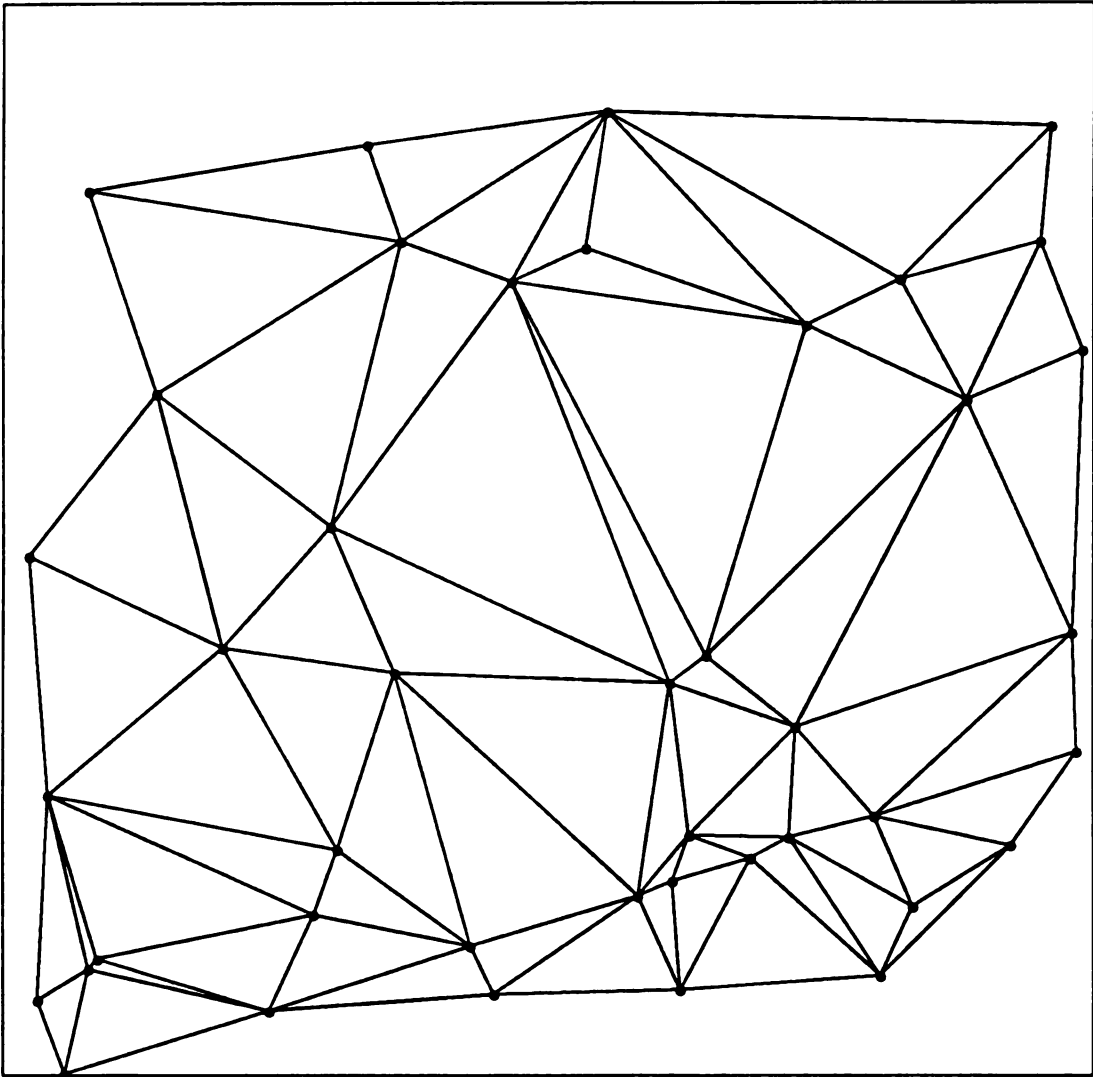


Figure 1-5 Delaunay Triangulation for Figure 1-3

The GG can be obtained from the DT by constructing a circle of influence for each DT edge. For each circle, the DT edge constitutes the diameter. Figure 1-6 gives two circles of influence used in obtaining the GG for Figure 1-3. If any dot falls within a circle of influence then the DT edge is removed, otherwise the DT edge is kept. In Figure 1-6, the large circle contains point P_{GG} therefore, the dotted DT edge AB defining the diameter is eliminated from the GG. The dashed DT edge CD defining the diameter of the small circle in Figure 1-6 is an edge of the GG because no image point falls within the circle of influence. To form the RNG, two circles are drawn for each DT edge with the centers at the endpoints and the radii defined by the length of the DT edge. The intersection of the two circles (lune) is the region of influence for the RNG. Figure 1-7 gives two lunes used to construct the RNG for Figure 1-3. If a lune contains no dots then the DT edge is retained, otherwise the DT edge is deleted. In Figure 1-7, the large lune is free of dots so the dashed DT edge GH remains part of the RNG. With the small lune of Figure 1-7, the point P_{RNG} causes the dotted DT edge EF to be eliminated from the RNG. The GG and RNG derived from Figure 1-5 are presented in Figures 1-8 and 1-9 respectively.

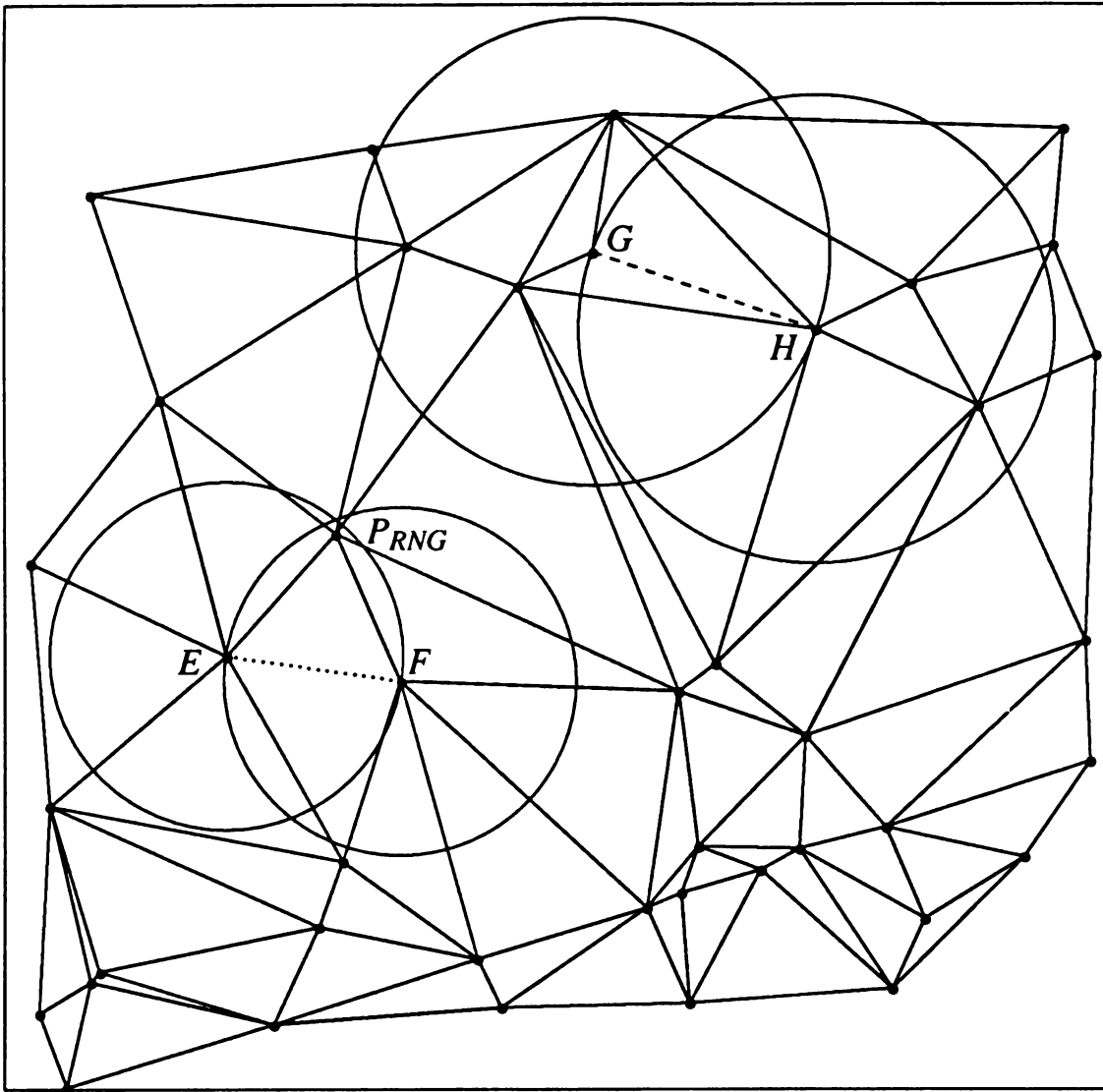


Figure 1-7 RNG Lunes of Influence. The dotted DT edge EF is deleted from the RNG because the point P_{RNG} is inside the lune created by the intersection of the two circles centered at E and F whose radii are defined by EF . The dashed DT edge GH remains part of the RNG because no point resides in the lune created by the intersection of the two circles centered at G and H with radii specified by GH .

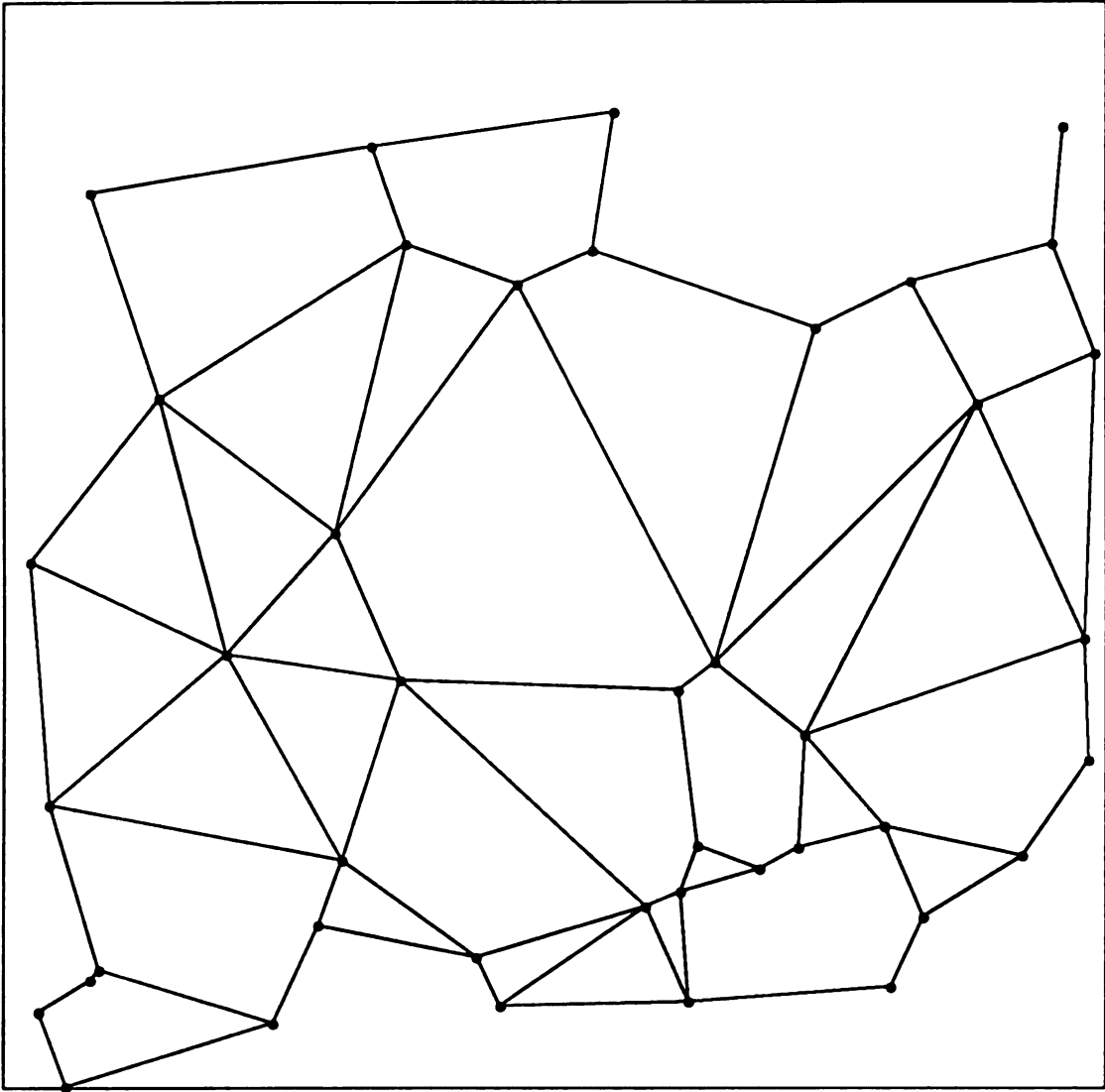


Figure 1-8 Gabriel Graph for Figure 1-3

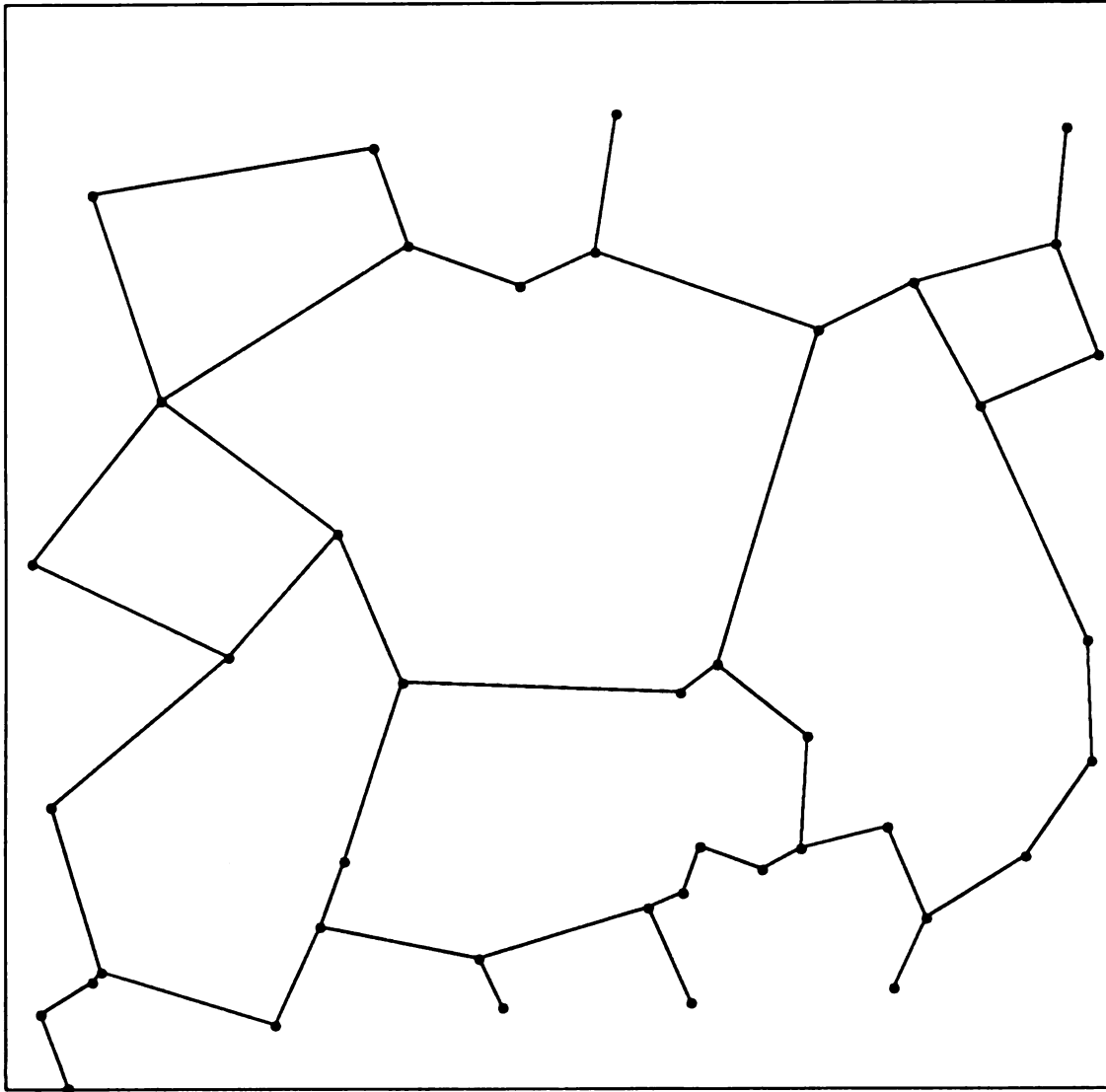


Figure 1-9 Relative Neighborhood Graph for Figure 1-3

The MST of a set of dots is formed by joining pairs of dots creating a tree that spans all dots such that the sum of the edge lengths is the minimum of all trees spanning the dot set. The MST is used in many fields and two classic MST algorithms are given in [KRU 56] and [PRI 57]. Since the MST is a subset of the DT, it can also be computed by only considering the edges of the DT [PRE 85]. Figure 1-10 is a MST of the dots in Figure 1-3.

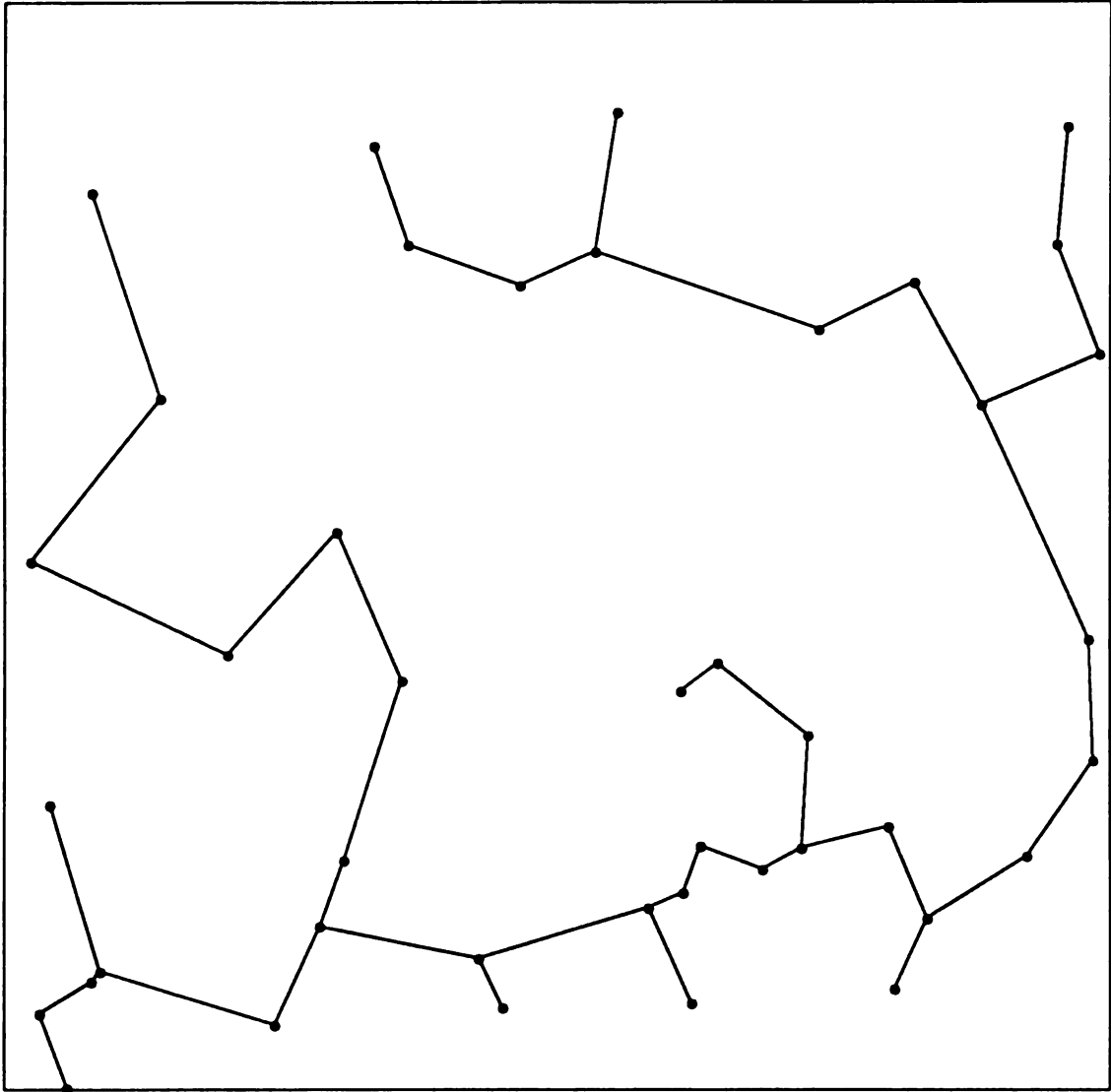


Figure 1-10 Minimum Spanning Tree for Figure 1-3

The reason for studying the DT, GG, RNG and MST is to assess the usefulness of each graph's neighbor relation in detecting structure in the presence of noise. The structure to be detected is linear and constructed of dots. This linear structure is embedded in a uniformly distributed random dot pattern which tests how robust the neighborhood of each graph is. When a graph is computed for the entire image, the noise points disrupt the graph edges that would join the dots of the line if no noise were present. To further test the stability of each graph's neighborhood definition, the dotted line is subjected to various types of perturbations. At some high level of distortion, none of the four graphs are expected to maintain the neighbors of the dotted line when surrounded by noise.

The type of dotted structure studied in this thesis is linear. The dotted line detection ability of each graph is determined by the fraction of the dotted line retained after it is embedded in a noisy background. In the case of the MST, a noise point in the vicinity of a dot which forms part of the line to be detected can cause a MST edge joining two dots on the line to disappear. This characteristic tends to make the MST sensitive to noise. With the less sensitive DT, it is more difficult to break an edge because a node of the DT has a less restrictive neighborhood definition than a node of the MST. In order to capture each graph's ability to retain the neighbors of the original structure in the presence of noise, a quantitative measure is needed. This measure must penalize a graph for allowing a line point to become isolated by losing neighbors belonging to the line and gaining neighbors that are considered part of the background. This process causes segments of the line to disappear. The measure must also allow noise points to strengthen the structure without any penalty assessed to the graph.

This situation arises when a noise dot falls on a graph edge joining two points of the line. Various combinations of line point perturbations are used in order to determine when a particular graph may completely break down and fail to retain the neighbor relations of the structure.

An important aspect of structure detection is how stable the graph neighbor information is. For instance, if two images of the same scene differ by small changes in the background then the differences in the neighbor information given by the graph should be proportional to the severity of the change. With the more global nature of the MST, it is expected that a small perturbation in the position of a dot will generate a disproportionately large change in the MST of the entire image. The DT vertex however has its neighbors defined as those points whose Voronoi polygons share an edge, therefore if a vertex is moved slightly then the DT is expected to change very little when compared to the MST.

In order to evaluate each graph's structural stability, one dot of a random dot pattern is perturbed. The perturbed dot is always the centermost dot of the image. Graph stability is measured by the highest order neighbor that has its vertex adjacencies modified. The order of a vertex that is a neighbor of a point is the minimum number of graph edges that connect the point and the neighbor. Directions of the perturbations are randomly selected. It is desirable that the graph's structure be well behaved for the neighbor information to be considered stable.

A major concern in using geometric methods is the time and space complexity of their calculation. Fortunately, efficient algorithms exist and can be easily implemented [GRE 78] [PRE 85] [PRI 57] [URQ 82]. Tous-saint [TOU 80A] provides a fairly complete survey of available algorithms.

1.2 Thesis Problem Statement

In this thesis, the DT, GG, RNG and MST will be employed to detect dotted linear structures which have been placed in uniformly distributed random dot patterns. A quantitative measure will be developed that reflects the degree of the dotted line remaining after the structure has been detected. The graphs will be ranked according to this quantitative measure. The emphasis will be on measuring each graph's behavior when controlled amounts of perturbation are applied to the structure dots. Only small amounts of variation will be examined. The types of perturbation are restricted to interdot spacing of the line, longitudinal variation from a dot's equally spaced position and transverse variation perpendicular to the line.

This thesis will also subject random dot patterns to perturbations of the centermost dot to determine the structural sensitivity of the DT, GG, RNG and MST. The highest order neighbor that has its vertex adjacencies altered will be recorded. The graphs will be ordered according to this neighbor order. The emphasis will be on measuring each graph's behavior when controlled amounts of distortion are applied to the centermost dot. Only small amounts of variation will be studied with the direction selected randomly.

1.3 Thesis Outline

Chapter Two reviews geometric applications to pattern recognition. Chapter Three outlines the methodology of this thesis and the quantitative measures computed. Chapter Four presents the results along with analyses. Finally, Chapter Five summarizes the thesis and gives suggestions for future work.

Chapter 2

Structure Detection

Computer vision and structural grouping have a very short history. As noted by Toussaint [TOU 80A], in the brief existence of pattern recognition few problems have been attacked using geometric structures despite their natural applicability. This chapter reviews some of the work already completed.

2.1 Background

The earliest attempt at defining the rules used in the perception of structure was reported by Gestalt psychologists [KOF 35] [WER 38]. They observed that the human vision system uses rules such as proximity, similarity, continuity, closure and symmetry in analyzing images. These criteria are helpful in explaining the perceptions of various images. Unfortunately, the Gestalt laws of perceptual grouping are only explanatory and do not shed light on the mechanisms that implement these rules.

Work concerning the implementation of the Gestalt laws in computer vision systems was scarce for a long period of time after the Gestalt laws

first appeared. Zahn's classic clustering paper [ZAH 71] had a major impact on the application of Gestalt laws to problems encountered by vision researchers. Zahn proposed using the MST to embody the principle of proximity in cluster detection problems and demonstrated that the MST performed well in clustering arbitrary point sets. In one instance the performance of the MST was analyzed in the presence of small amounts of noise widely and randomly spread over the image. This thesis will explore the effects of noise on graph behavior more systematically.

Since the appearance of Zahn's paper, studies using various graphs in image analysis have become more frequent. Toussaint [TOU 80A] surveys many geometric structures that have been used in solving a variety of pattern recognition problems. In another paper, Toussaint [TOU 80B] introduces the RNG and espouses its usefulness in extracting perceptually meaningful structure from a set of points. Both papers presented no performance analysis of the geometric structures and offered numerous directions for future research.

A proposal for applying another type of geometric structure to pattern recognition problems is given by Ahuja [AHU 82]. Here he argues that the Voronoi tessellation gives a better definition of a point's neighborhood than methods using parameters that need to be tuned according to the input point pattern. As in Zahn's work, Ahuja goes on to define the Voronoi tessellation along with its attributes and presents numerous instances where the Voronoi neighborhood works well. Later, Ahuja's ideas were expanded upon in [TUC 86].

Another example of geometric applications to pattern recognition is presented by Urquhart [URQ 82]. Urquhart gives a general family of

graphs defined by using a region of influence which includes the GG and RNG. He presents point patterns where these region of influence graphs do well in locating clusters. Urquhart does provide some comparative results of the MST, GG and RNG to show their viability but the analysis is not extensive.

Numerous other instances of complex pattern recognition problems addressed by geometric methods can be found. A good survey of results is given by [TOU 87] accompanied by an extensive bibliography.

Chapter 3

Methodology

The objective of this thesis is to determine the relative performance of the DT, GG, RNG and MST in two areas of computer vision. One concern is the effect of interdot spacing, longitudinal variation and transverse variation on each graph's line detection capability. Also of concern is each graph's structural sensitivity to single point perturbations. This chapter describes the methodology employed and the experiments performed.

Section 3.1 presents the problem under study. Section 3.2 elaborates on the procedure and Section 3.3 gives the performance measures. Finally, Section 3.4 specifies the parameters studied in each of the six experiments.

3.1 Problem to Study

As implied earlier, the rationale behind using graphs for structure detection is based on the neighbor relationship they induce on the image entities. Figures 1-5, 1-8, 1-9 and 1-10 show how graph edges between dots are eliminated from the DT to the MST based on the changing neighborhood definitions. For instance, the MST with its strict constraints on

node adjacencies (relative to the DT), groups nodes together that are within close proximity to one another. In a vision setting, image points can be separated into figure points and noise points based on their surrounding environment. Figure 3-1 displays a dotted structure and its MST. In the absence of background noise all the points of the structure are MST neighbors. Figure 3-2 adds uniformly distributed noise to Figure 3-1. When the MST of Figure 3-2 is computed, only a small subset of the points of the original structure are MST neighbors. The presence of noise in Figure 3-2 causes the original MST neighbors of the line in Figure 3-1 to be modified resulting in a deterioration of the line into segments.

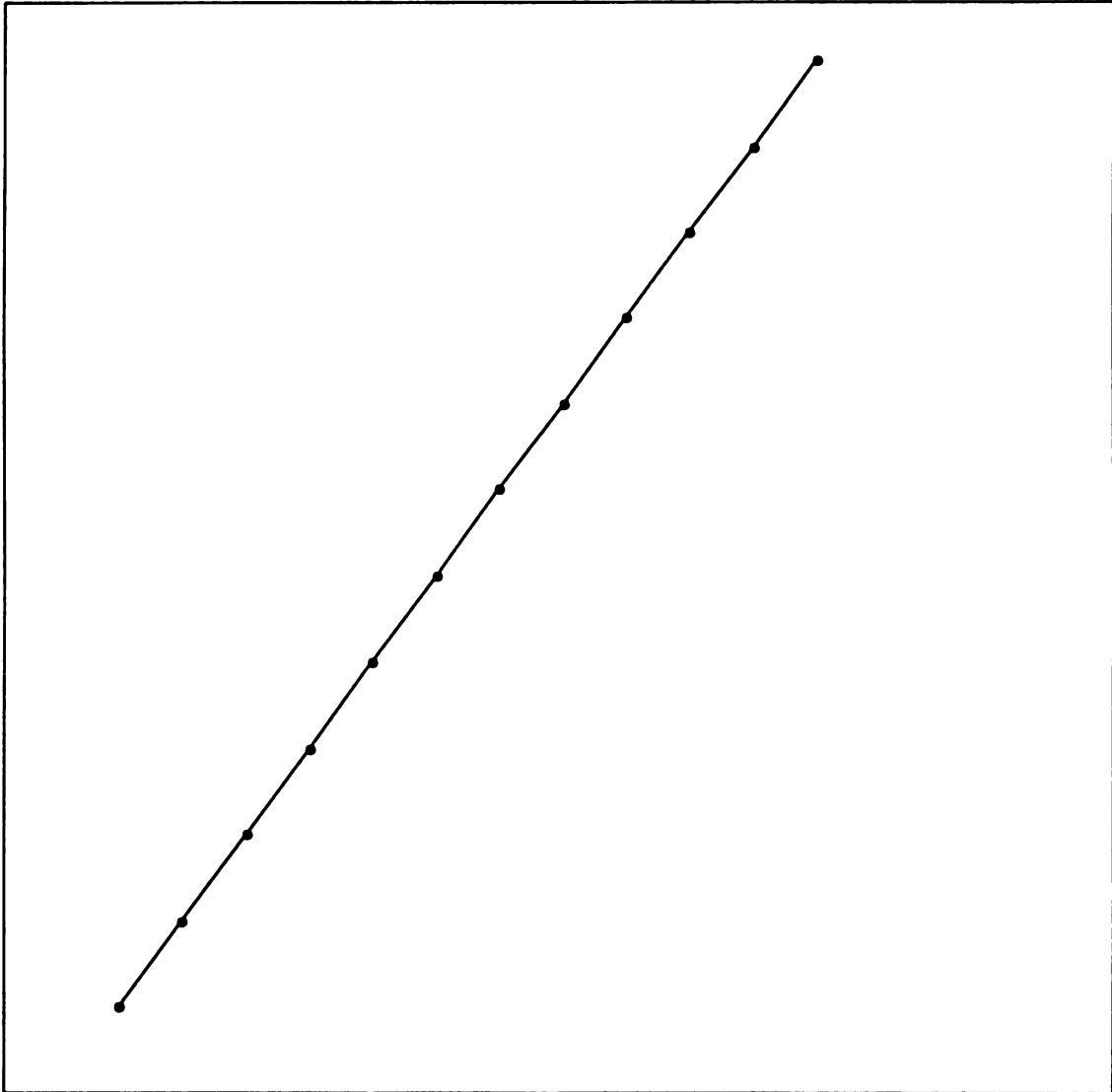


Figure 3-1 MST of a Dotted Line

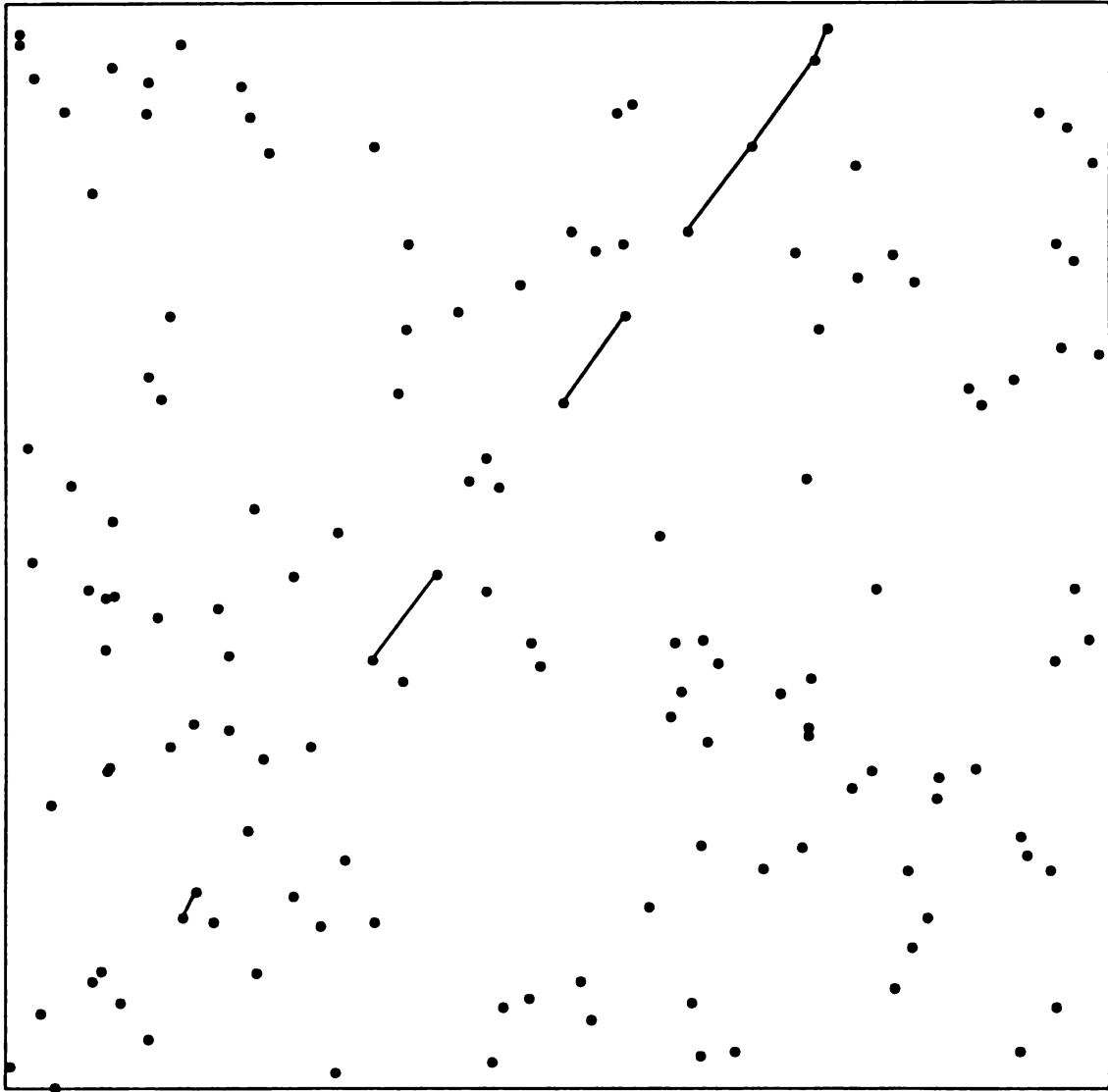


Figure 3-2 MST of a Dotted Line Surrounded by Noise

More specifically, one problem under consideration is the detrimental effect that dot perturbations have upon a graph's ability to maintain the node adjacencies of a structure in a noisy environment. The structures under consideration here are simple and consist of dotted lines. Three types of perturbations are explored: interdot spacing, longitudinal variation and transverse variation. By varying the spacing of the dots comprising a structure, the dots once perceived as part of the structure are now considered part of the background. In the case of interdot spacing, a closely spaced dotted line is capable of blending into the background as the interdot spacing of the line nears the interdot spacing of the surrounding environment. For human visual perception, this was shown experimentally by Vistnes [VIS 87]. Figure 1-2 contains a structure whose interdot spacing is larger than the average interdot distance of the background. A measure is employed to quantify how well a graph resists this structure disappearance by retaining the connections between the dots of the original structure.

The second problem under consideration is the effect of single dot perturbations on the structure of the DT, GG, RNG and MST. The dot perturbations consist of varying the position of the centermost dot in a random direction and identifying the vertices of the graph that have their vertex adjacencies altered. The order of the vertex that has its neighbors changed is used to quantify how stable the graph's structure is. To be considered stable, the graph should limit the effect of the change and reflect the magnitude of the change in a proportional manner.

3.2 Procedure

The structure detection procedure employed in this thesis consists of three stages, (i) image generation with controlled structure variations, (ii) Hough transformation which detects global structures present in the image, and (iii) identification of local structures by imposing graph adjacency relationships on the global structures obtained by the Hough transform. The graph stability procedure consists of two stages, (i) image generation and (ii) identification of the highest order neighbor effected by the image dot perturbations.

3.2.1 Generation of Structure Detection Images

This step generates a uniformly distributed random dot pattern according to an average interdot distance parameter and then randomly places a dotted line within this uniform background. The dotted line is of random position and orientation and possesses specific interdot spacing and variation characteristics. The background noise dots are generated in the same manner as in [VIS 87] with the number of background noise dots described by one parameter, an average interdot distance D . A Poisson distribution of noise dots is approximated by a normal distribution N with the mean equal to the variance. The mean number of noise dots used for N is computed by

$$\frac{A}{D^2}$$

where A is the area of the image.

The normally distributed random numbers of N used to approximate the Poisson distribution of the background dots are produced using the polar coordinate method [BOX 58] [MAR 62]. First, two uniformly

distributed random numbers between 0 and 1 are converted into two uniformly distributed random numbers between -1 and +1. Let U_1 and U_2 represent the two uniformly distributed random numbers between -1 and +1 and set $V = U_1^2 + U_2^2$. If $V \geq 1$ then the procedure is restarted. Otherwise, the normally distributed random numbers of N are obtained by evaluating the expression below.

$$N = U_1 \sqrt{(-2 \ln V) / V}$$

Dot placement within the image is uniform. The x and y coordinates of each dot are generated by multiplying a uniformly distributed random number between 0 and 1 by the length of an image boundary.

The uniform random number generator used is the lagged Fibonacci (17,5,-) [GEB 67] generator. The lagged Fibonacci generator is first seeded by 17 uniformly distributed random numbers from a linear congruential random number generator which is itself seeded by one prime number. Uniformly distributed random numbers between 0 and 1 are now produced by $X_i = X_{i-17} - X_{i-5}$ for $i = 18, 19, 20, \dots$.

The dotted line parameters are interdot spacing, longitudinal variation and transverse variation. Figure 3-3 defines these three parameters where S is the interdot spacing, L is the longitudinal variation and T is the transverse variation. Note that the range of L is from $(-0.5)S$ to $(+0.5)S$. Systematic variation of these parameters allows the study of each graph's sensitivity in detecting structure that has not been explored in previous work. The L and T dot perturbations are determined by two uniformly distributed random numbers from the lagged Fibonacci generator. The first random number selects the perturbation direction. One direction is

designated by numbers between 0.0 and 0.5 inclusive and the other direction is designated by numbers greater than 0.5. The amount of the perturbation is calculated by multiplying the second random number by the perturbation parameter. In the case of L , the second random number is halved before the multiplication.

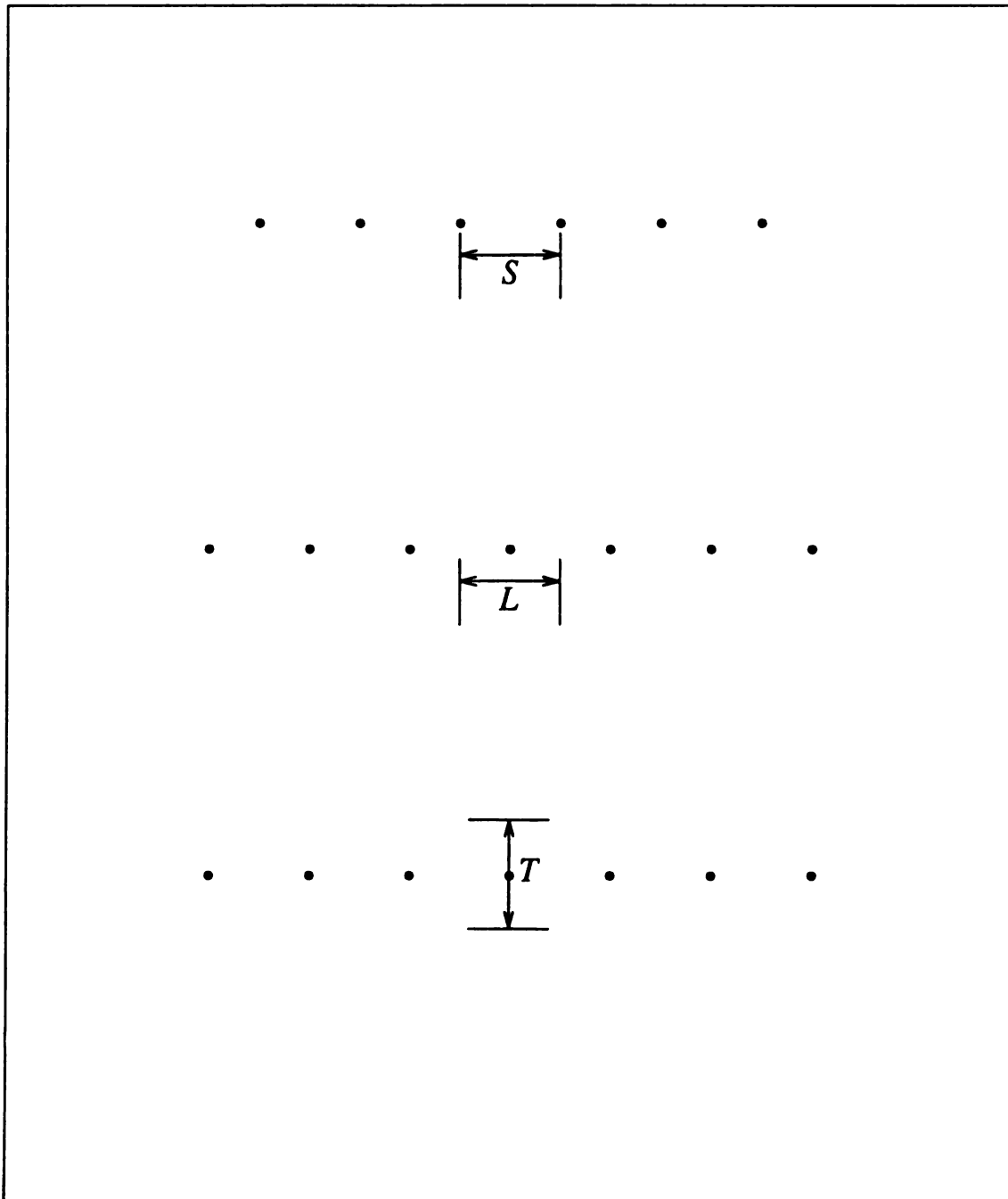


Figure 3-3 *Spacing, Longitudinal and Transverse Variations.* Dots comprising the line to be detected are perturbed in three ways. *Spacing* dictates the interdot distance of the line and *Longitudinal* perturbation alters the location of a dot along the line with respect to the dot's equally spaced position. Finally, *Transverse* perturbation moves a dot in a direction perpendicular to the line.

3.2.2 Detection of Global Structure

The Hough transformation [HOU 62] has been studied extensively [BAL 81] [BRO 83] [CAS 87] [DUD 72] [ILL 87] [MAI 86] [SHA 79] [SKL 78] [VAN 81] and is a well known global technique for detecting structures in images. In stage two, the Hough transform is used to locate linear structures in the image. The parameterization proposed by Duda and Hart [DUD 72] is implemented here to avoid difficulties with infinite slope. Basically, the Hough transform performs a mapping of lines from the image space to the parameter space. The equation of a line l can be given as

$$\rho = x \cos \theta + y \sin \theta \quad (1)$$

where ρ and θ are the parameters defining l as shown in Figure 3-4. For a fixed point (x,y) , equation (1) defines all the lines that pass through the point and creates a sinusoid in the (ρ,θ) space. So, given the (x,y) coordinate pair of an image dot, θ is varied from 0 to 360 degrees producing a series of (ρ,θ) Hough cell coordinates specifying the Hough cells to be incremented. In essence, the (x,y) coordinate pair votes for a number of lines, each represented by the (ρ,θ) Hough cell coordinates. After this voting process is completed for all the image dots, the Hough cell with the highest count has the (ρ,θ) coordinates that determine the line in the image space having the largest number of dots. Since the line points can be perturbed transversely, a band surrounding the line [MAI 86] is used to determine the figure and noise points representing the detected line. Figure 3-5 shows the points of a typical image that fall within such a band around a detected line. The points of the detected line are then used to decrement the Hough cells in a manner analogous to incrementing the Hough cells.

That is, the (x,y) coordinate pair of every image dot on the detected line is applied to equation (1) and the (ρ,θ) coordinates of the Hough cells to decrement are given by varying θ from 0 to 360 degrees. When the decrementing procedure is completed for all the line dots, a new maximum Hough cell emerges resulting in the next detected line. This process is repeated until the maximum Hough cell count equals two. Lines made up of two points need not be considered because any two points constitute a line. Note that there is no thresholding to eliminate noise lines.

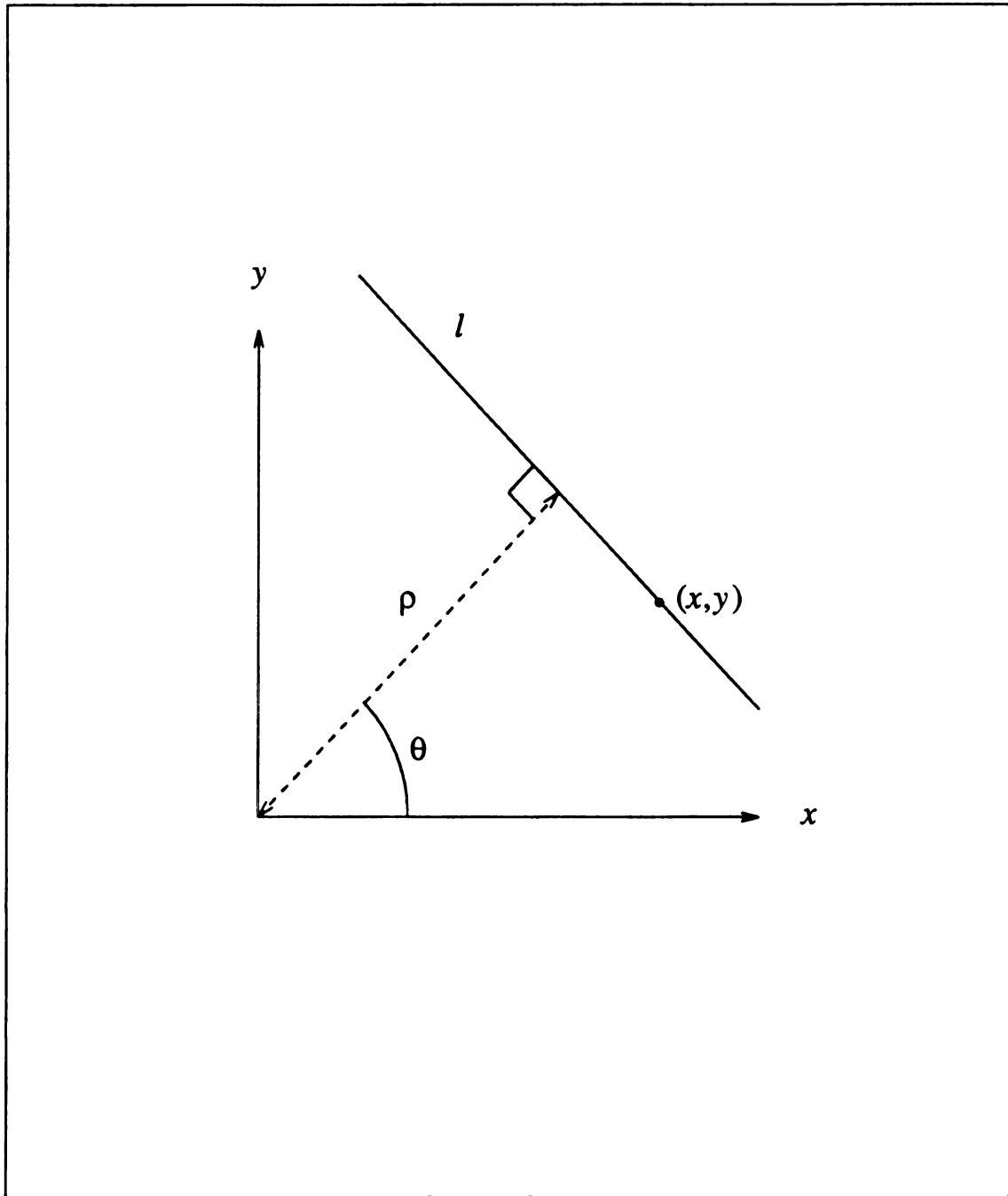


Figure 3-4 Hough Parameters of a Line. The line l is defined by the equation $\rho = x \cos \theta + y \sin \theta$ with parameters ρ and θ . The length of the normal from the origin to l having (x, y) as a point is the radius ρ . The angle the normal forms with respect to the x axis is θ .

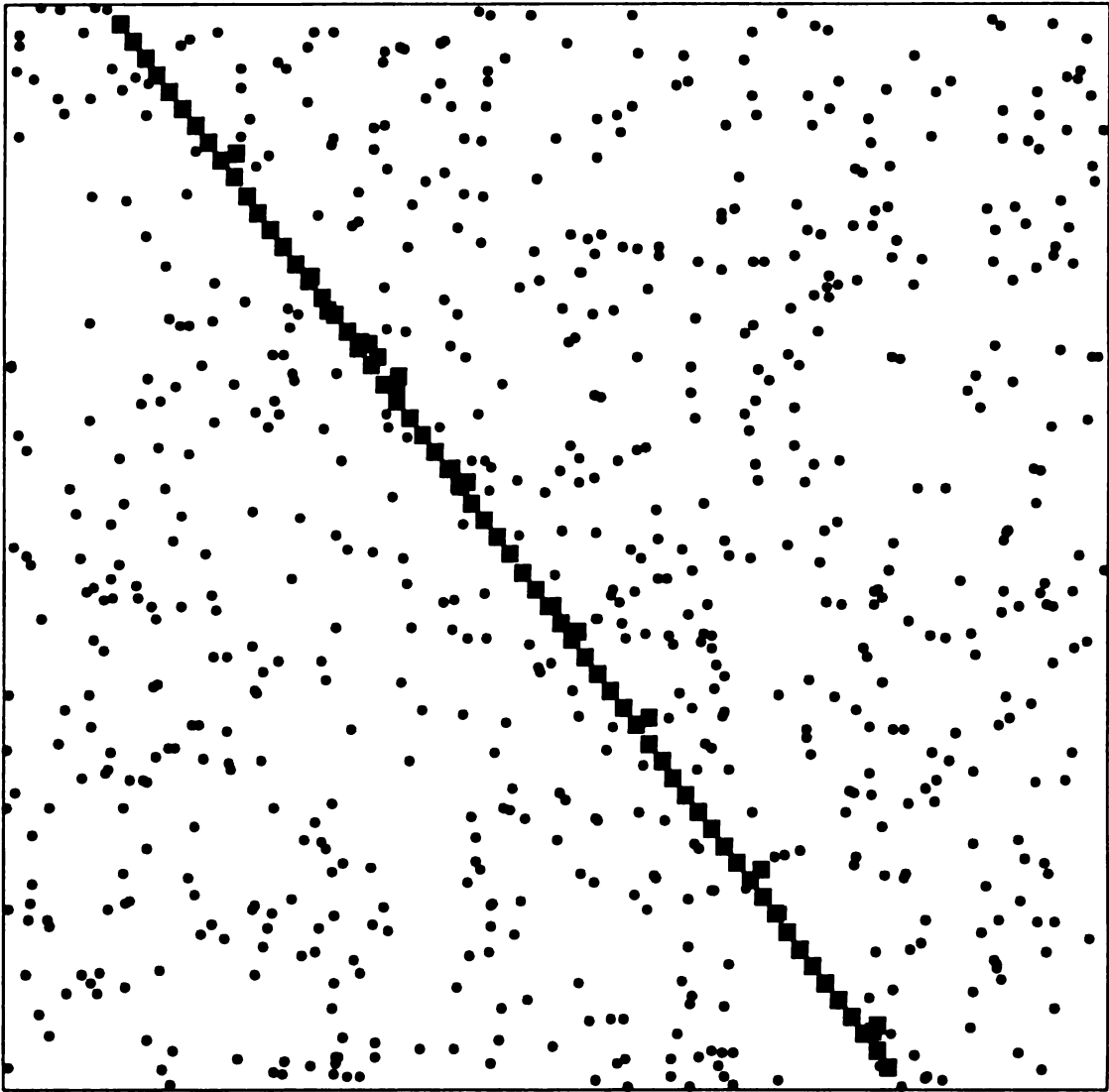


Figure 3-5 Points of a Hough Detected Line. After identifying the Hough cell with the highest count, a band surrounding the line specified by the (ρ, θ) Hough cell coordinates is used to locate the image dots belonging to the line.

3.2.3 Localizing the Structure using Graphs

The third and final stage of the structure detection procedure involves determining which points of the structure detected by the Hough transform method are neighbors. This neighbor relation is defined by the four different graphs. Step three shows how the different graph neighbor relations effect the graph's structure detection capability. For example, a MST neighbor is a point that is the closest whereas a DT neighbor has no such requirement.

For each line detected by the Hough method, a two dimensional neighbor matrix is formed where the rows and columns represent the points of the line. An entry in the matrix is made if two line points are neighbors of one of the four graphs computed for the entire random dot pattern. The reflexive, symmetric and transitive closure of this dot neighbor matrix is then obtained using Warshall's algorithm [WAR 62]. This computation produces groups of points that form connected components. The points of every connected component are now intersected with the points of the original dotted line. The resulting connected components made up of the original line points are finally compared to the original structure in order to determine the portion of the line that is retained by each graph.

3.2.4 Generation of Graph Stability Images

Images used for determining each graph's structural stability are produced in the same fashion as the images used for determining each graph's structure detection ability. The only difference is that no dotted line is implanted. The dot perturbation parameter specifies the variation amount that is added to the x and y coordinates of the centermost dot. The direction

of the x and y variation is dependent on two uniformly distributed random numbers from the lagged Fibonacci generator. A number between 0.0 and 0.5 inclusive represents a positive direction and a number greater than 0.5 represents a negative direction. Systematically varying the perturbation amount allows the study of how well each of the graphs respond to the change.

3.2.5 Identification of Altered Neighbors

The last stage of the graph stability procedure involves determining the highest order neighbor whose vertex adjacencies have changed due to the movement of the centermost dot. This step shows the graph's structural reaction to small changes in the position of image entities.

First, the DT, GG, RNG and MST are computed for the entire image. After the centermost dot is perturbed, the DT, GG, RNG and MST are then recomputed using the perturbed image. The original graph and the perturbed graph are now compared, edge by edge starting from the centermost dot, to locate any differences. When a difference is found then the neighbor order is recorded. The order of a vertex that is a neighbor of the centermost dot is the minimum number of graph edges that connect the centermost dot and the neighbor. Figure 3-6 is an example of the first, second and third order DT neighbors of the centermost dot in a uniformly distributed random dot pattern.

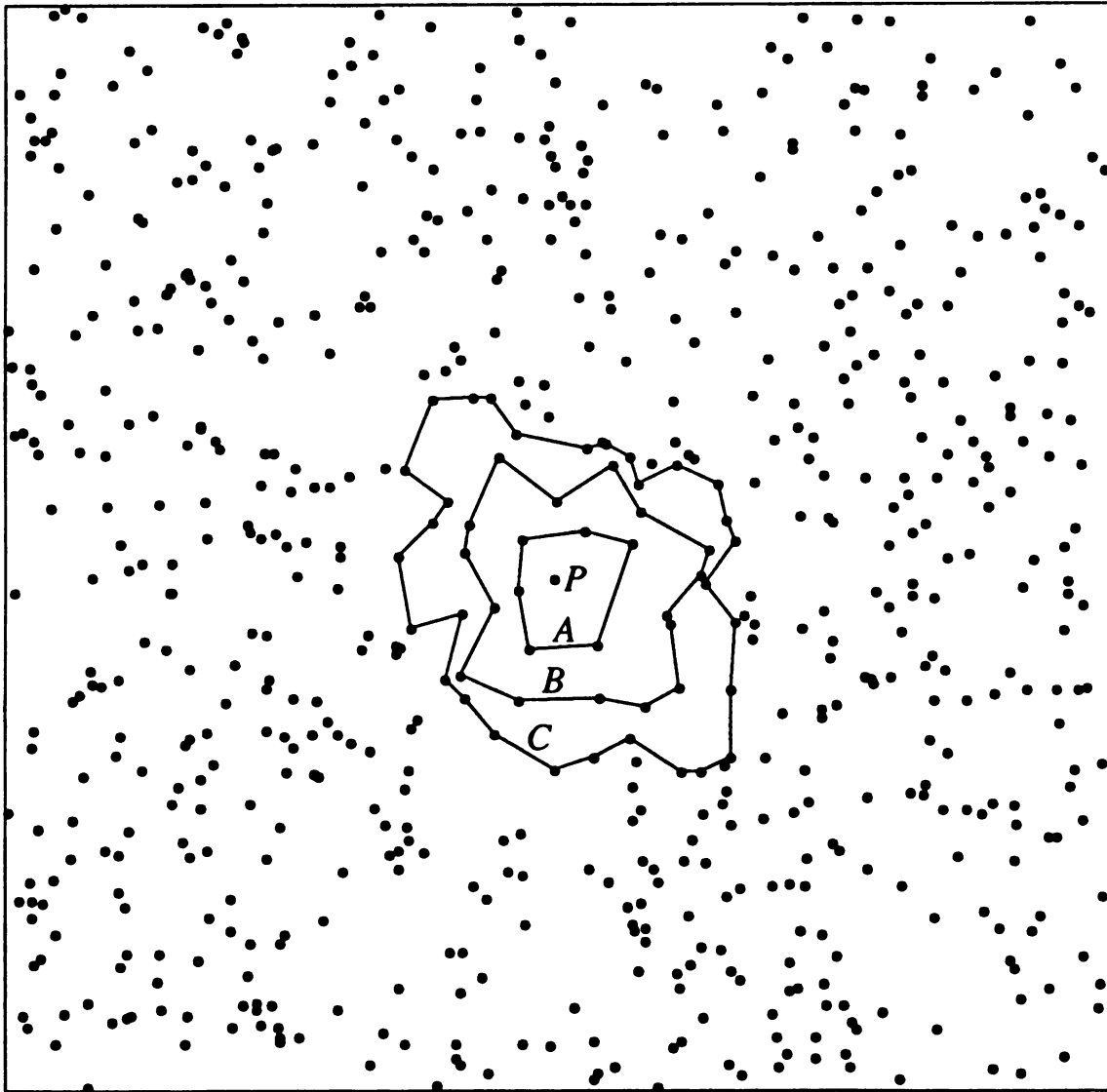


Figure 3-6 First, Second and Third Order DT Neighbors. The set of points on curve A are the first order DT neighbors of the centermost point P . The points on curve B are the second order DT neighbors of P and the points on curve C are the third order DT neighbors of P .

3.3 Measures of Sensitivity

One measure, a figure significance, is computed to rank each graph's relative performance in the linear structure detection task. The figure significance is the fraction of the structure's total retained MST length in the presence of noise compared to the structure's total MST length in the absence of noise. Let P_L be the set of points of the original line and let P_G be the set of points of a connected graph G . Let G_i for $i = 1, 2, 3, \dots, m$ be the set of all connected components remaining at the end of the structure detection procedure. Now defining $L(P)$ as the total length of the MST for the point set P , the figure significance measure is computed by the following equation.

$$\text{Figure Significance} = \frac{\sum_{i=1}^m L(P_{G_i} \cap P_L)}{L(P_L)}$$

Therefore, a figure significance of 1.00 is the maximum and corresponds to all points on the structure being neighbors according to a particular graph neighbor relation. At the other extreme, a figure significance of 0.00 is the minimum and corresponds to every point of the structure having no graph neighbors.

The measure used to determine each graph's relative structural stability is the highest order of the neighbors whose adjacencies have changed due to the perturbation of the centermost dot. This vertex order is an indication of the severity of the change in the graph's structure.

3.4 Experiments

Four experiments were performed to evaluate each graph's structure detection sensitivity. All experiments were run with a 512 by 512 square grid. Each experiment consisted of five prime numbers to initialize the random number generator and produced five distinct images with identical control parameters from which the figure significance measurements were obtained then averaged. Within each of the five images, one randomly generated dotted line is embedded with varying degrees of perturbation under the control of the three variation parameters (interdot spacing, longitudinal variation and transverse variation). Limits on the line spacing were imposed based on the Vistnes ratio [VIS 87]. This ratio compares the interdot spacing of the figure to the average interdot distance of the background. Vistnes has shown that a ratio of 1.10 is the point where the figure is no longer perceivable by humans due to the background interference. Transverse variation was also limited to avoid creating bars (two dimensional objects) instead of lines. Finally, experimental measurements were discarded when the Hough transformation did not locate the embedded structure. That is, if the Hough transform detected a line whose position and orientation did not match the target line then the figure significance of such a failure is ignored when computing the averages.

Two experiments were performed to evaluate each graph's structural stability to single dot perturbations. Both experiments were run with a 512 by 512 square grid. Each experiment consisted of 100 prime numbers to initialize the random number generator and produced 100 distinct images with identical control parameters. With each of the 100 images, the center-most dot is perturbed in a random direction and in increasing amounts. The

maximum perturbation amount is again limited by the Vistnes ratio [VIS 87] of 1.10. For each perturbation, the highest order of the neighbors effected is averaged over the 100 uniformly distributed random dot images.

For the graph stability experiments, a measurement significance Z is computed using a confidence coefficient of 0.95 and the following formula.

$$Z = \frac{(\mu_1 - \mu_2)}{\left[\frac{\sigma_1^2}{N_1} + \frac{\sigma_2^2}{N_2} \right]^{\frac{1}{2}}}$$

Here μ_1, μ_2 represent the sample means, σ_1^2, σ_2^2 signify the sample variances and N_1, N_2 give the number of samples taken from the two populations. A $|Z| > 1.96$ indicates the difference between the sample means μ_1 and μ_2 is significant with a confidence level of 95%. The measurement significance is computed using the average neighbor order of the DT and every other graph. Therefore, μ_1, σ_1^2 and N_1 are the mean, variance and number of samples respectively for the DT at each perturbation amount and μ_2, σ_2^2 and N_2 are the same quantities for one of the other graphs under the same perturbation parameter.

Experiment 1 - Spacing (20)

A set of images are generated each of which contains one evenly spaced dotted line of random position and orientation embedded in a background of uniformly distributed random dots. The average interdot distance of the background noise is 20 pixels. Line spacing is varied from 10 pixels (one half the average interdot distance of the background) to 22 pixels (1.10 times the average interdot distance of the background) in increments of three pixels. For each line spacing, five random dot images are

generated and the figure significance measurements are averaged over these five images. It is expected that as the line spacing increases, the graphs will detect less of the dotted line.

Experiment 2 - Spacing, Transverse (20)

In this experiment, transverse variation as well as line spacing is varied. Line spacing is varied from 10 pixels to 22 pixels in increments of three pixels. For the transverse variation, a dot on the line is randomly perturbed from plus or minus two pixels to plus or minus four pixels. For each set of perturbation values, five random dot images are generated and the figure significance measurements are averaged over these five images. Again, the additional distortion is expected to hamper the graph's structure detection capability and increase the interference caused by the background noise.

Experiment 3 - Spacing, Longitudinal, Transverse (20)

This experiment introduces every possible dot variation combination. For each combination, there are five random dot images generated containing one dotted line of random position and orientation. Line spacing is varied from 10 pixels to 22 pixels in steps of three pixels. A dot is randomly perturbed longitudinally from its evenly spaced position, either forward or backward, up to a maximum of one half of the interdot spacing of the line. Experiment 3 explores longitudinal variations of plus or minus three, six and nine pixels. The dots are then subjected to transverse variations of plus or minus two, three and four pixels with the perpendicular direction selected randomly. Experiment 3 should provide a rigorous test

of each graph's structure detection potential.

Experiment 4 - Spacing, Longitudinal, Transverse (16)

The parameters in this experiment are exactly the same as Experiment 3 except that the background noise has been increased by decreasing the average interdot distance from 20 pixels to 16 pixels. Because of the decrease in the average interdot distance of the background, the maximum line spacing need only be 19 pixels instead of 22 pixels. Results of Experiment 4 should mirror the results of Experiment 3.

Experiment 5 - Perturbation (20)

Experiment 5 contains 100 images with the average interdot distance equal to 20 pixels. The position of the centermost dot is altered in steps of three pixels starting from 3 pixels to a maximum of 21 pixels. The direction of the variation is randomly selected. For each perturbation amount, the highest order of the neighbors effected is averaged over the 100 random dot images. Experiment 5 is expected to show increasing average neighbor orders as the dot perturbation amount gets large.

Experiment 6 - Perturbation (16)

The parameters in this experiment are exactly the same as Experiment 5 except that the dot density of the image has been increased by decreasing the average interdot distance from 20 pixels to 16 pixels. Due to the decrease in the average interdot distance of the image, the maximum dot variation need only be 18 pixels instead of 21 pixels. The results of Experiment 6 should replicate those of Experiment 5.

Chapter 4

Results and Discussion

The results of the six experiments are presented in this chapter. The first four experiments involve the analysis of the effect of various perturbations on a graph's structure detection ability in the presence of noise. The last two experiments involve the analysis of single dot perturbations on a graph's structural stability. Results are presented graphically along with a discussion and some example images. Note that the curves depicting the outcome of Experiments 1, 2, 5 and 6 do not represent continuous functions but related measurements joined by line segments to emphasize their behavior.

4.1 Experiment 1 - Spacing (20)

In this first structure detection experiment, the simplest type of variation is tested. As Figure 4-1 illustrates, it is very easy to perceive the embedded structure. The line is immediately obvious because the dot spacing of the structure is one half the average interdot distance of the background. This fact is responsible for the corresponding high average figure

significance values of Figure 4-2 at a line spacing of 10 pixels. All four graphs perform well at this spacing, connecting the closely spaced dots and detecting the associated structure direction suggested in [ROS 73]. Figure 4-3 and Figure 4-4 give the MST and DT neighbors of the structure in Figure 4-1 and reflect the high average figure significance measurements by maintaining the majority of connections between the structure dots. Referring again to Figure 4-2, graph structure detection performance begins to decline as the interdot spacing of the line increases. Note the gap between the DT and the MST at the line spacing of 19 pixels indicating that the MST is more strongly affected by the widely spaced structure points. The insensitivity of the DT is present throughout the range of line spacings. An important point in interpreting the experimental results is that the purpose of Experiments 1 through 4 is to ascertain trends in the graph's structure detection capability under the parameters tested by each experiment. Figure 4-5 shows the same line as Figure 4-1 but with a spacing just shy of the average interdot distance of the background. The increased difficulty in perceiving the dotted line of Figure 4-5 is reflected by the MST's inability to locate the complete line and is illustrated in Figure 4-6. Figure 4-7 gives the DT of the line in Figure 4-5 and still maintains the neighbors of the dots that make up the line. The lower than expected average figure significance values of Experiment 1 can be attributed to the band used in determining the image points of the Hough detected line. Here the band surrounding the line is of a fixed width and the line is located in the center. In Experiments 2, 3 and 4, the band is of the same fixed width but due to the transverse variation of the dots comprising the line, the band surrounds the line in a manner that results in the detection of the largest number of

points. Therefore, the results plotted in Figure 4-2 and Figures 4-9, 4-13 and 4-14 cannot be compared.

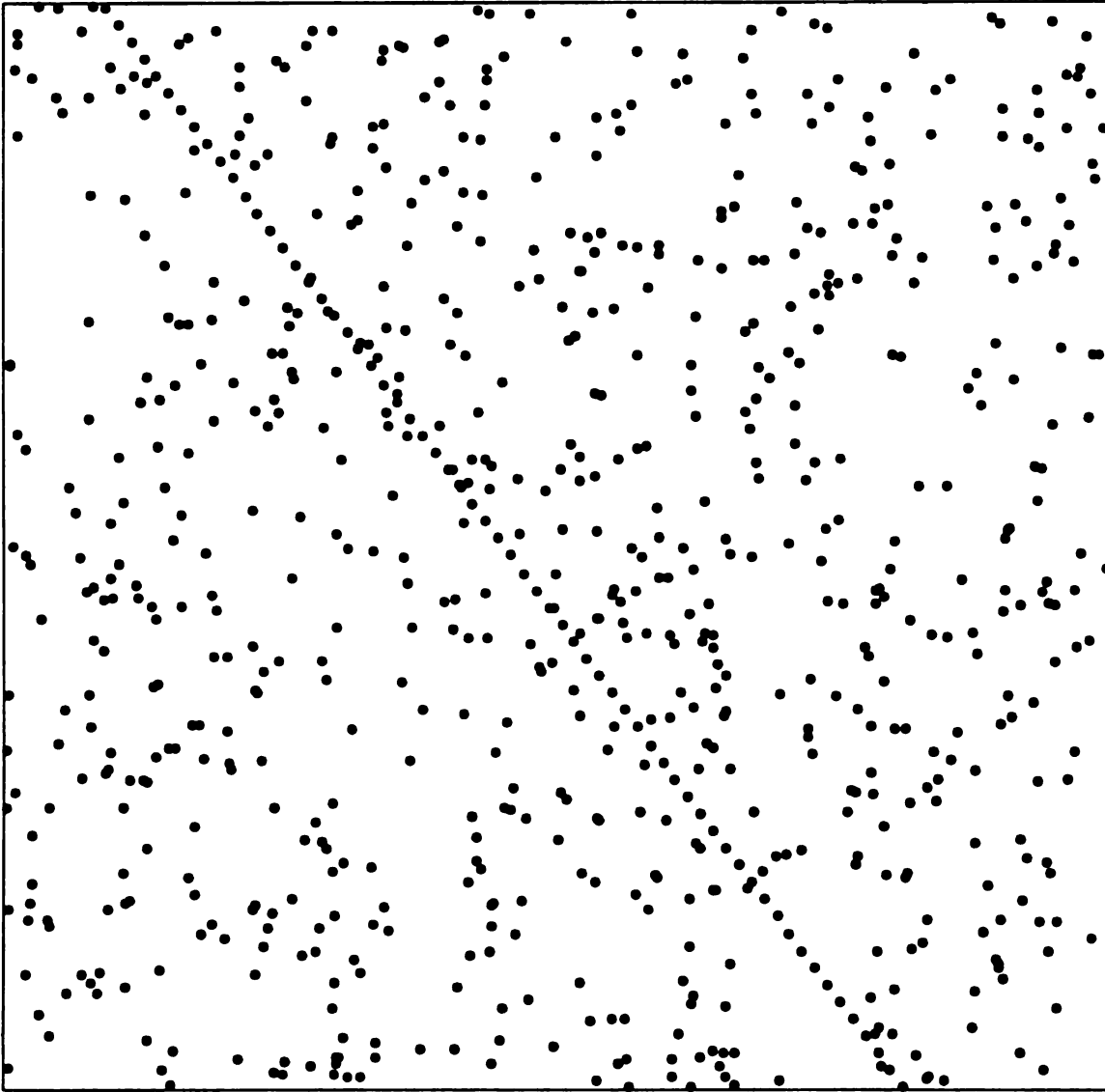


Figure 4-1 Experiment 1, Small Dotted Line Perturbations

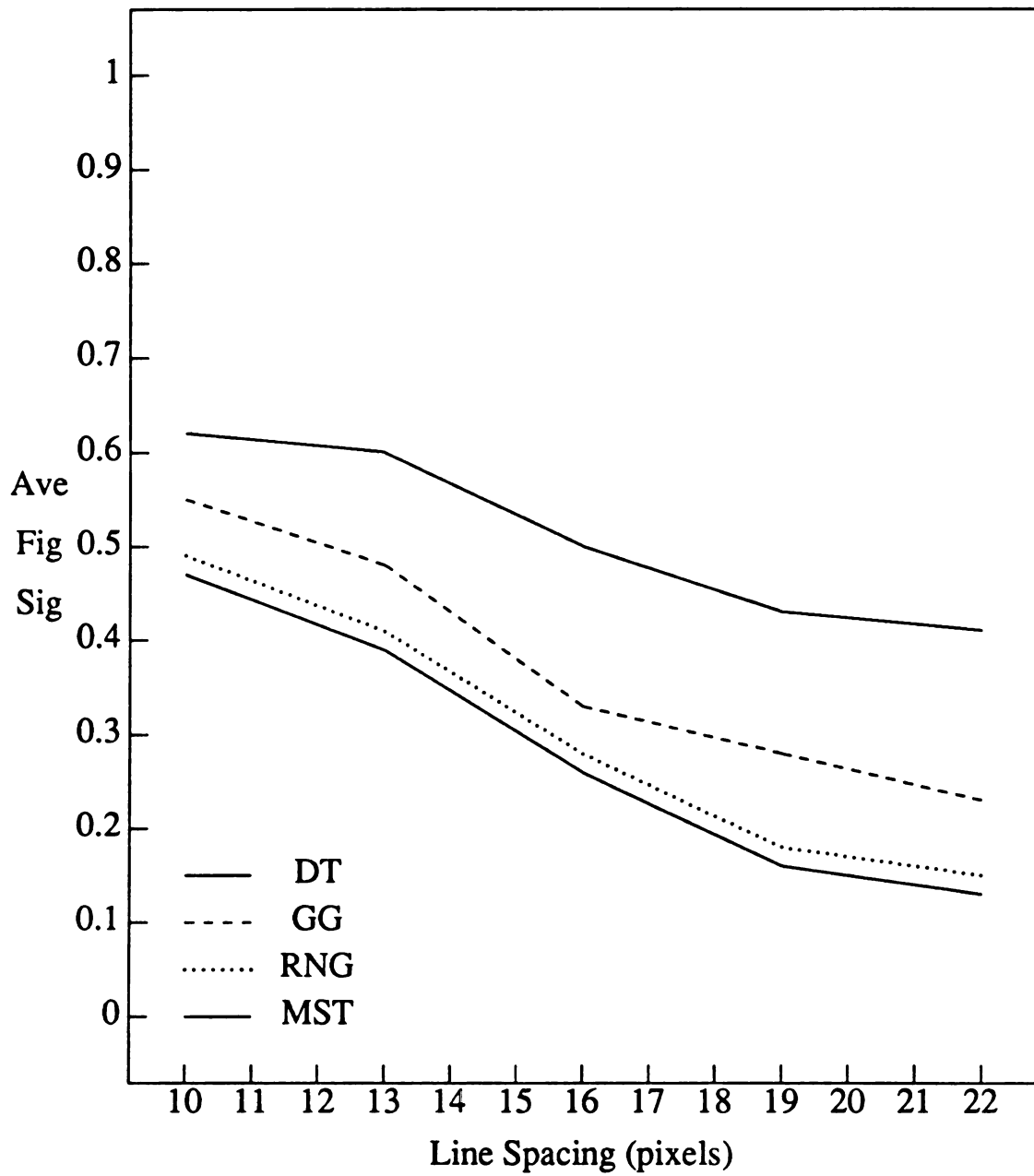


Figure 4-2 Experiment 1, Average Figure Significance Results

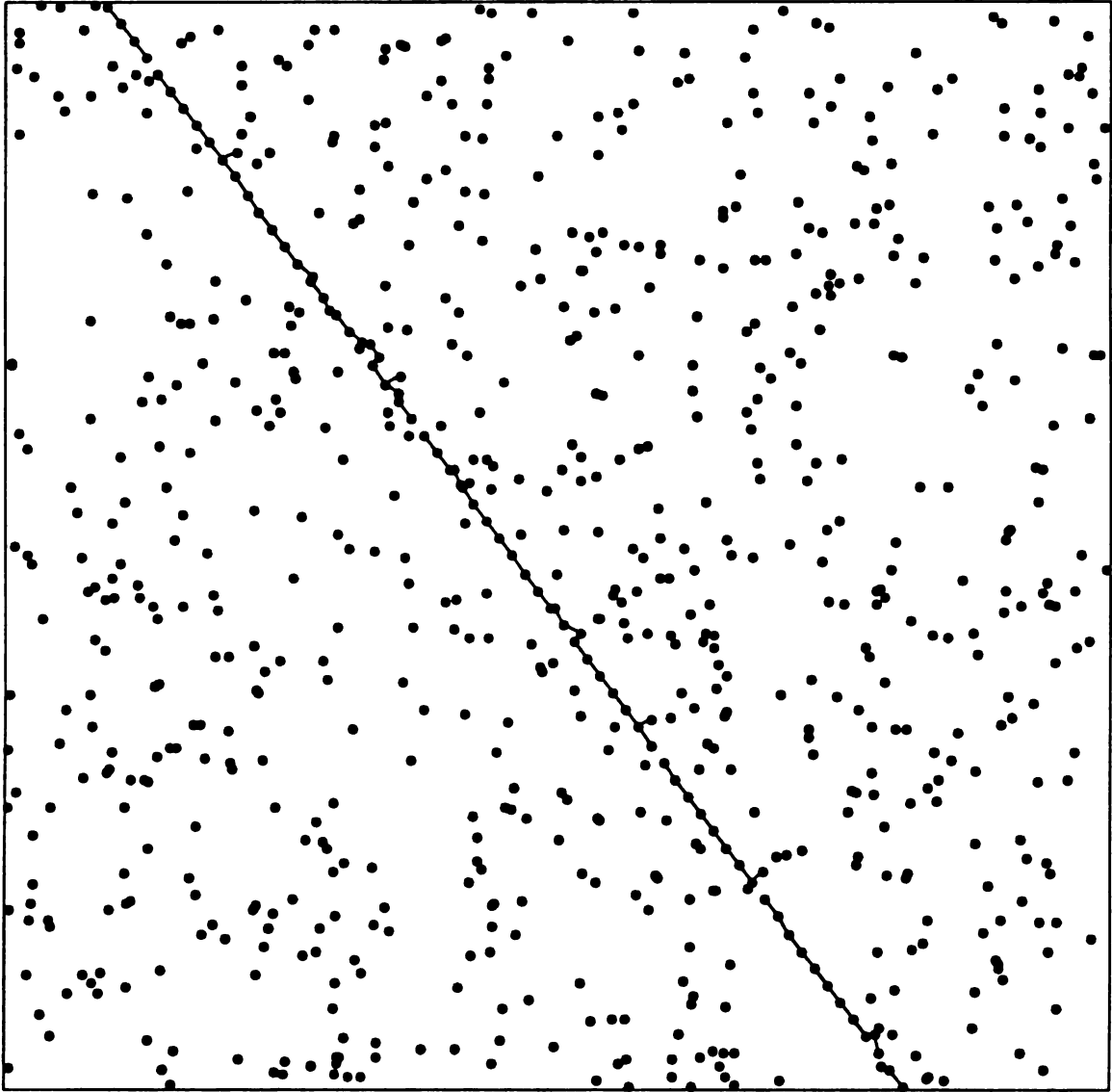


Figure 4-3 Experiment 1, MST of Small Dotted Line Perturbations

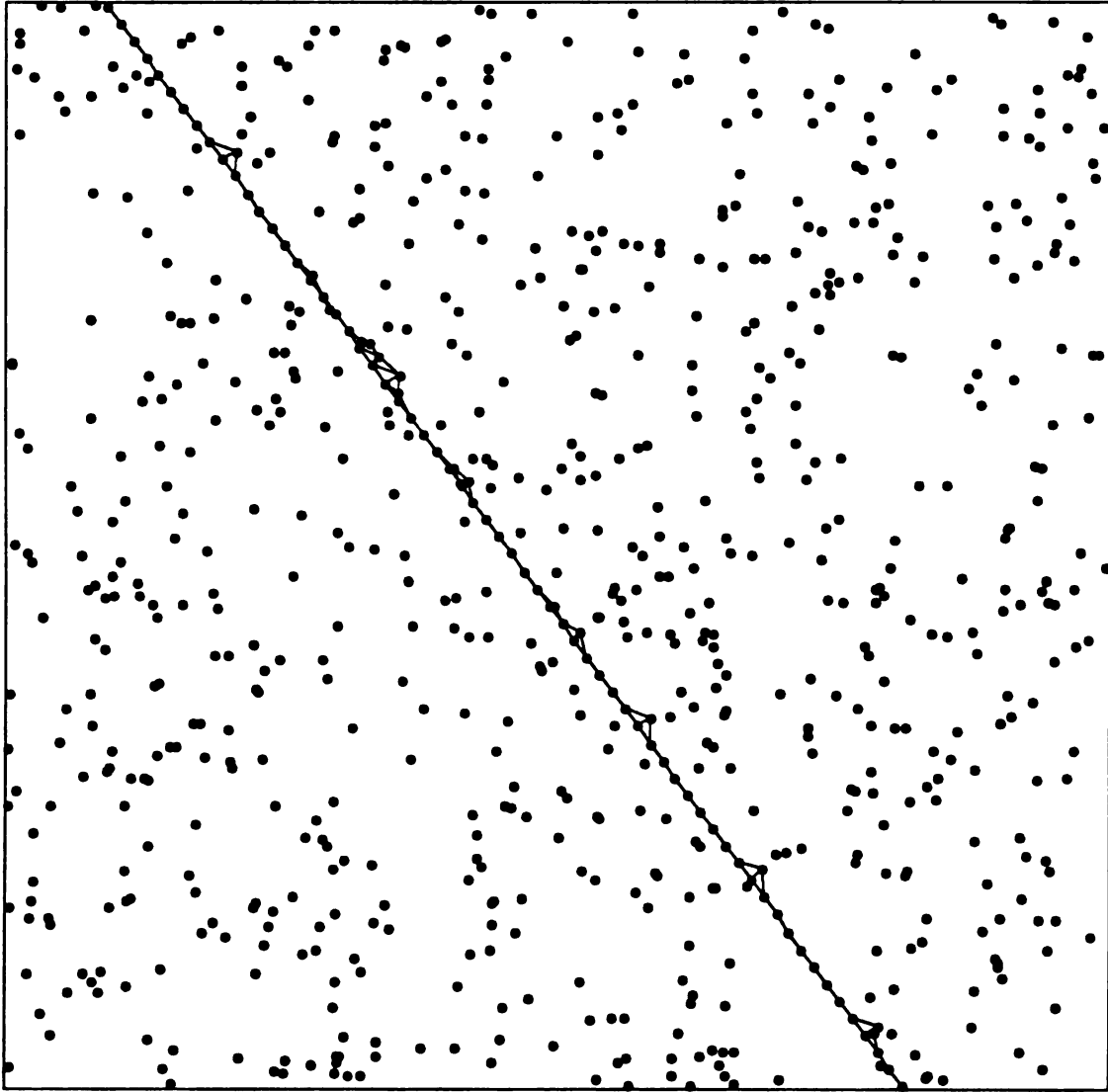


Figure 4-4 Experiment 1, DT of Small Dotted Line Perturbations

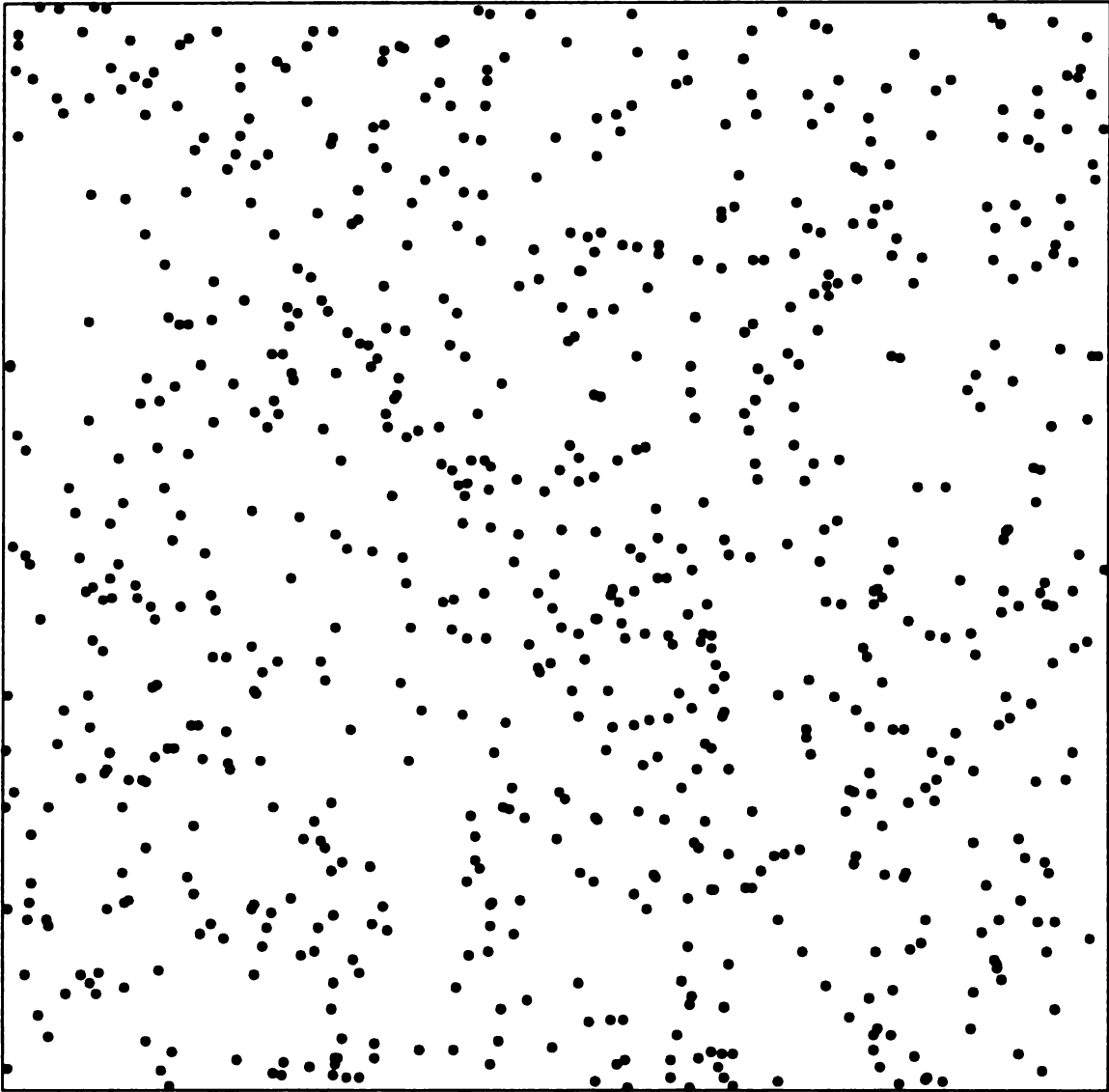


Figure 4-5 Experiment 1, Large Dotted Line Perturbations

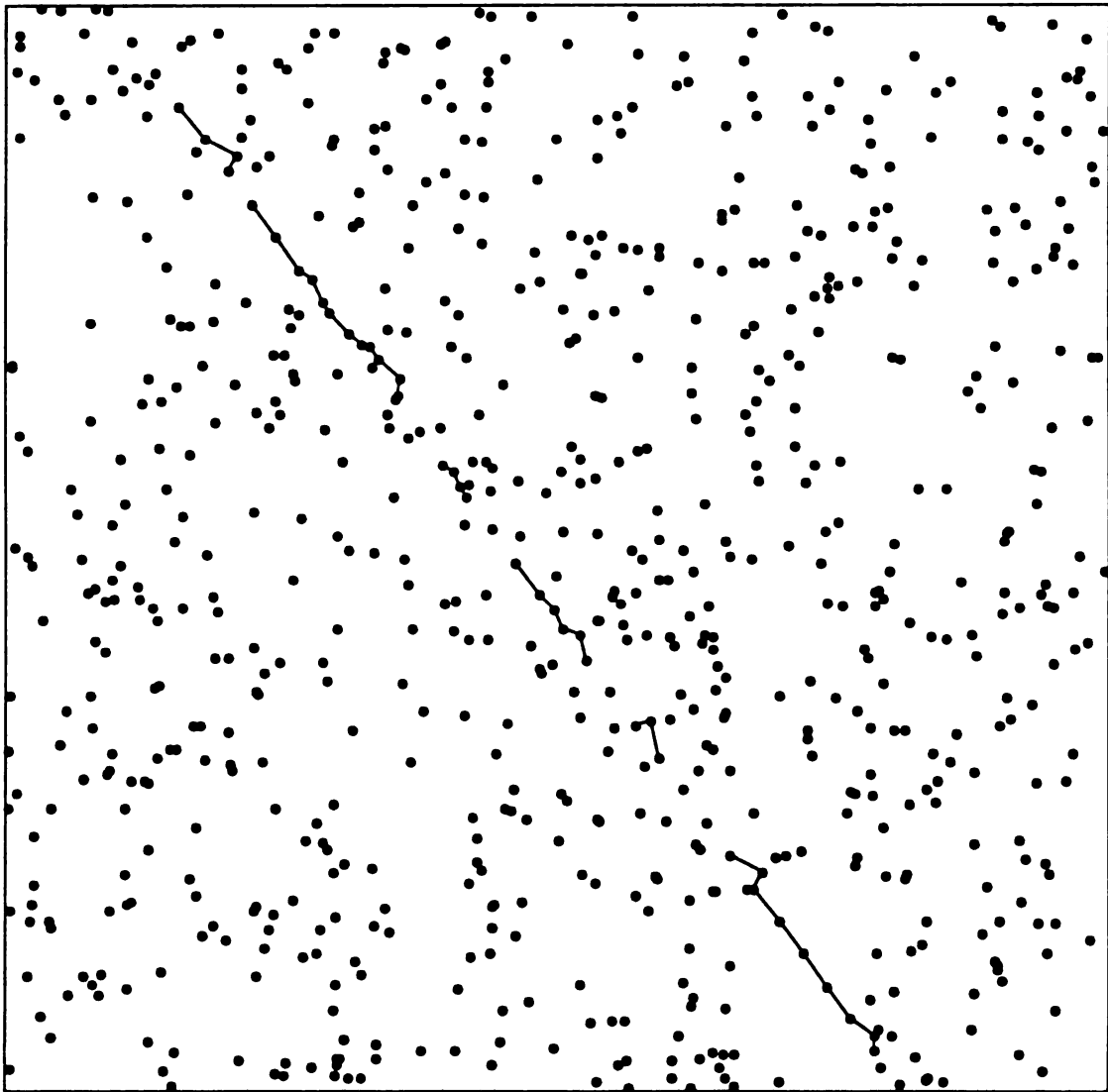


Figure 4-6 Experiment 1, MST of Large Dotted Line Perturbations

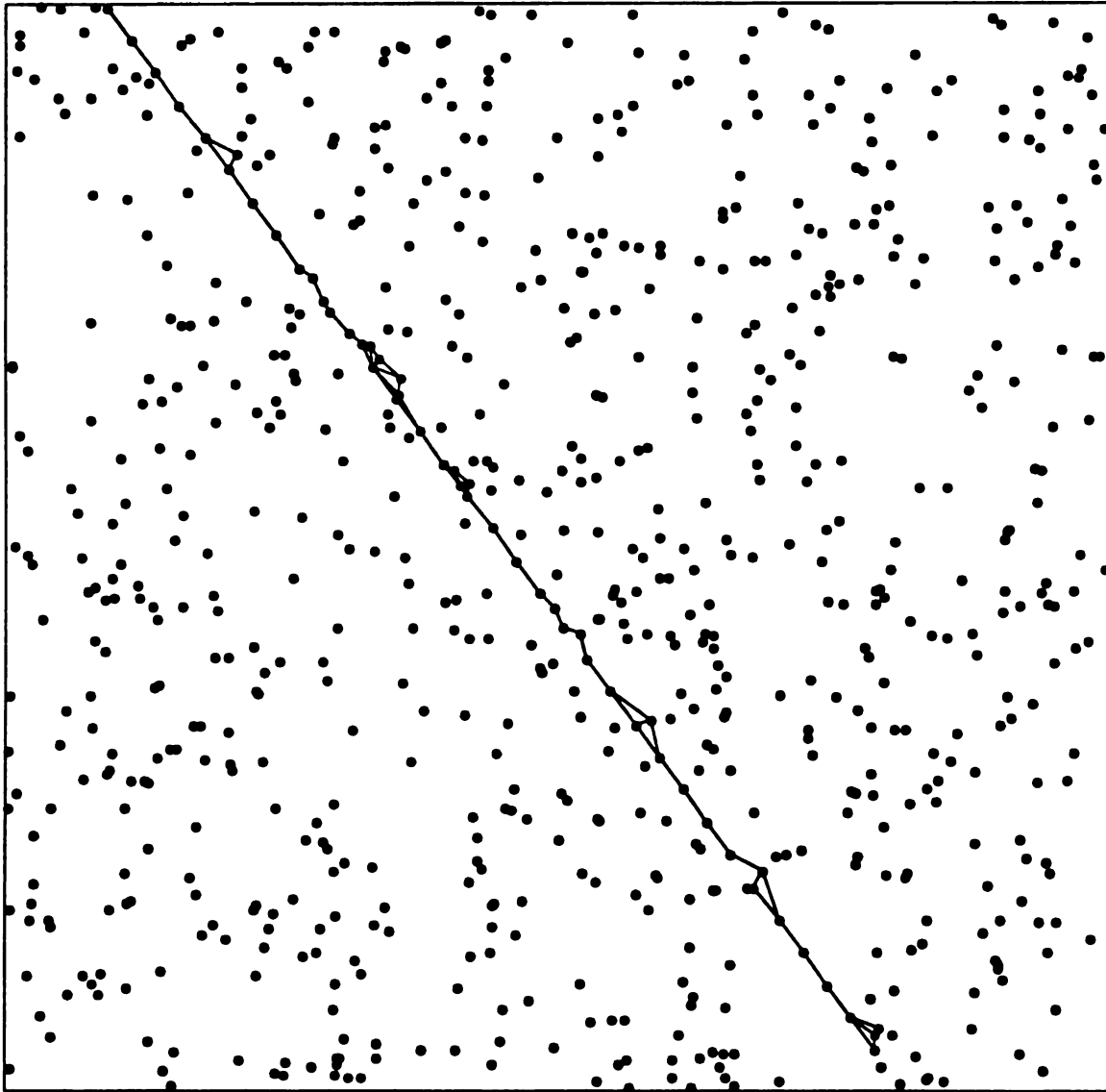


Figure 4-7 Experiment 1, DT of Large Dotted Line Perturbations

4.2 Experiment 2 - Spacing, Transverse (20)

Figure 4-8 is an example of the additional level of structure perturbation in Experiment 2. In this test, transverse variation has been introduced in increments of one pixel beginning with plus or minus two pixels and ending with plus or minus four pixels. Since Figure 4-8 does not contain large amounts of perturbation, it is still easy to perceive the line. The relatively high average figure significance measurements of the DT depicted in Figure 4-2 are again evident in Figure 4-9 with all four graphs performing well in the cases where the structure to background interdot distance ratio is small. Like Experiment 1, as the interdot spacing and transverse variation increase, all the graphs retain less of the line with the MST retaining the least and having the highest rate of disintegration regardless of the transverse perturbation amount. The sharp decline between the line spacings of 19 and 22 pixels is due to the small number of valid figure significance measurements used for the average. As pointed out earlier, figure significance measurements are discarded if the Hough transform fails to detect the target line. Figure 4-10 shows the same line as in Figure 4-8 except that the structure interdot spacing is nearly doubled. A decrease in the average figure significance measurements of Figure 4-9 accompanies the increased perturbation depicted in Figure 4-10.

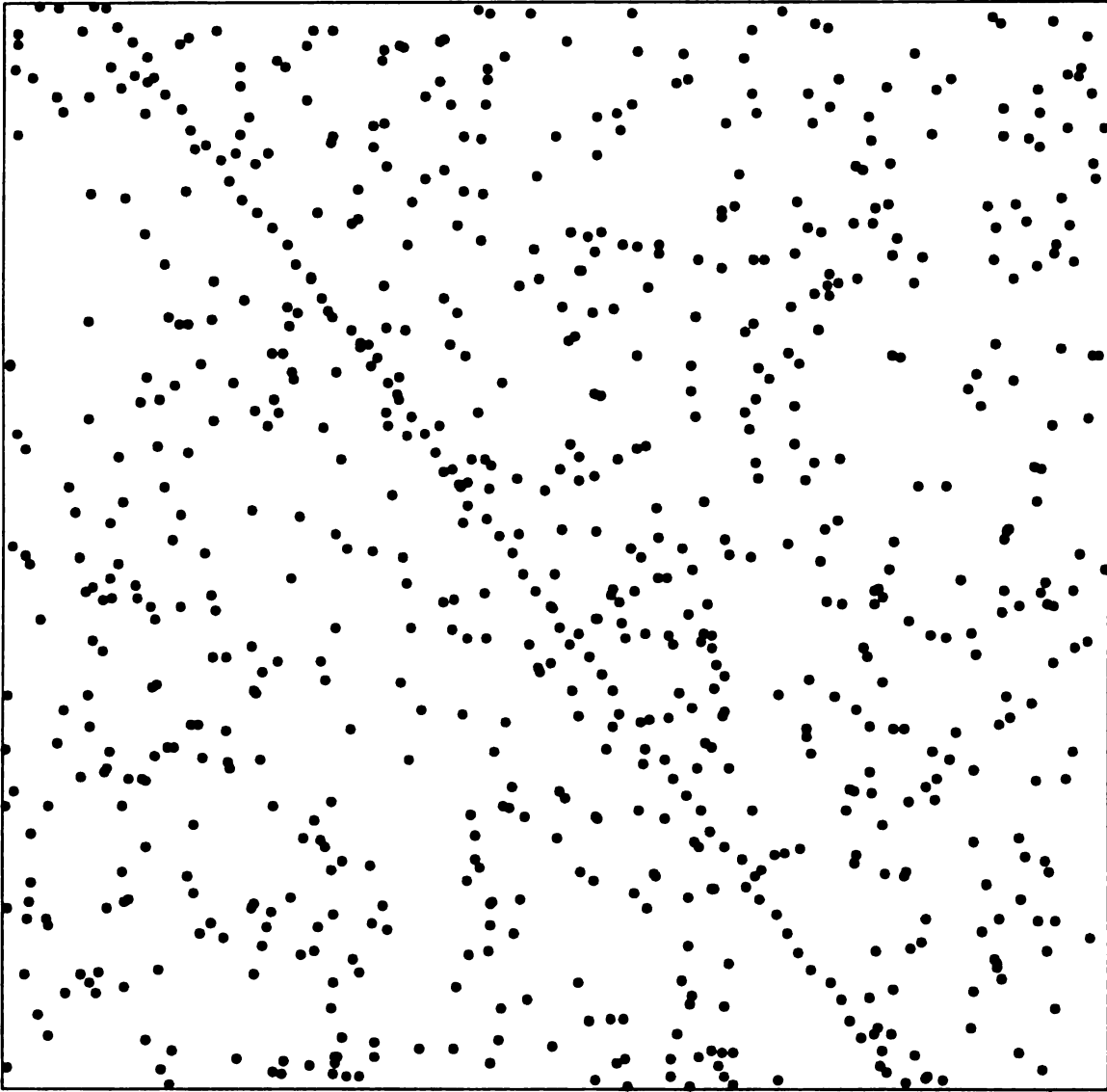


Figure 4-8 Experiment 2, Small Dotted Line Perturbations

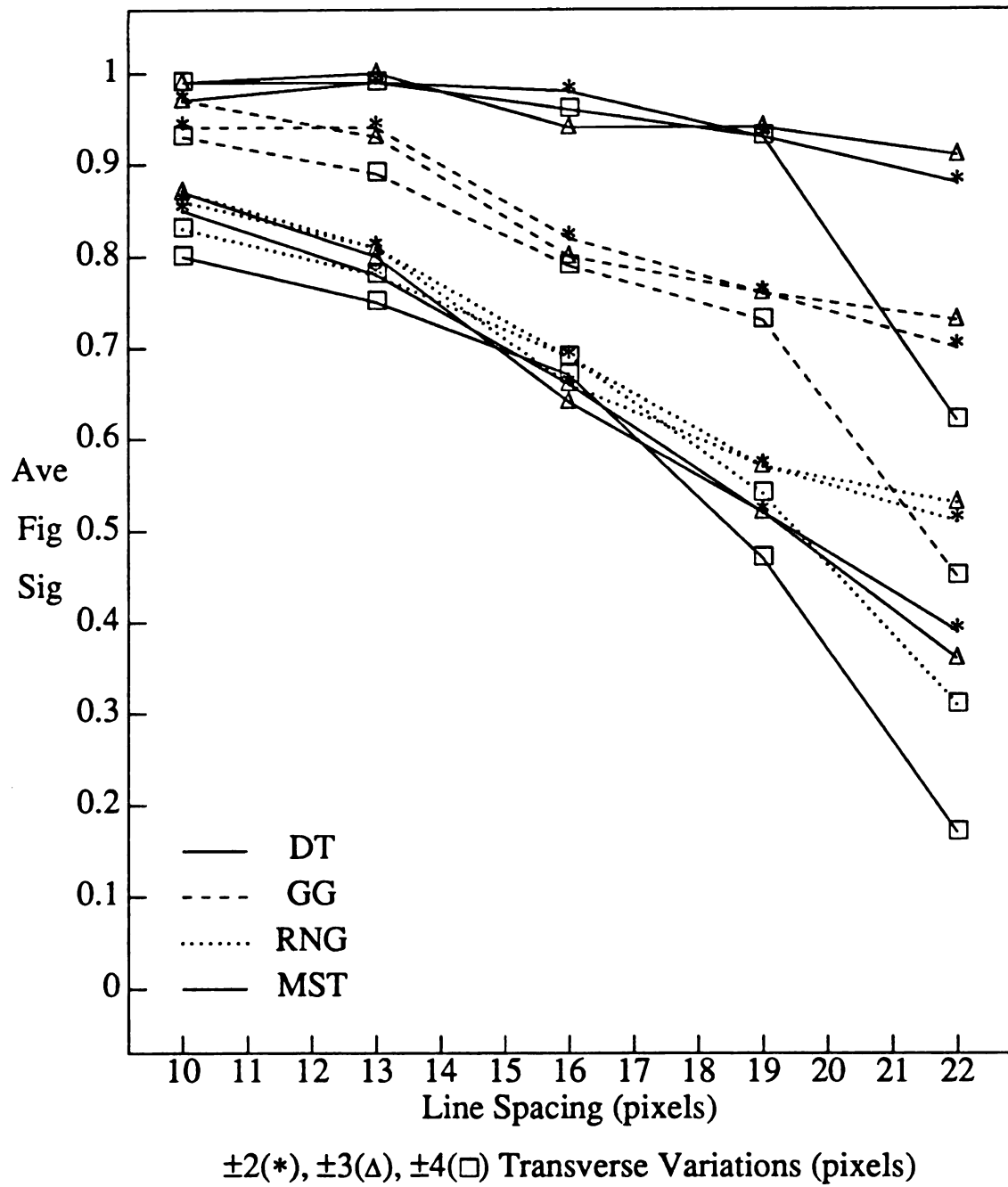


Figure 4-9 Experiment 2, Average Figure Significance Results

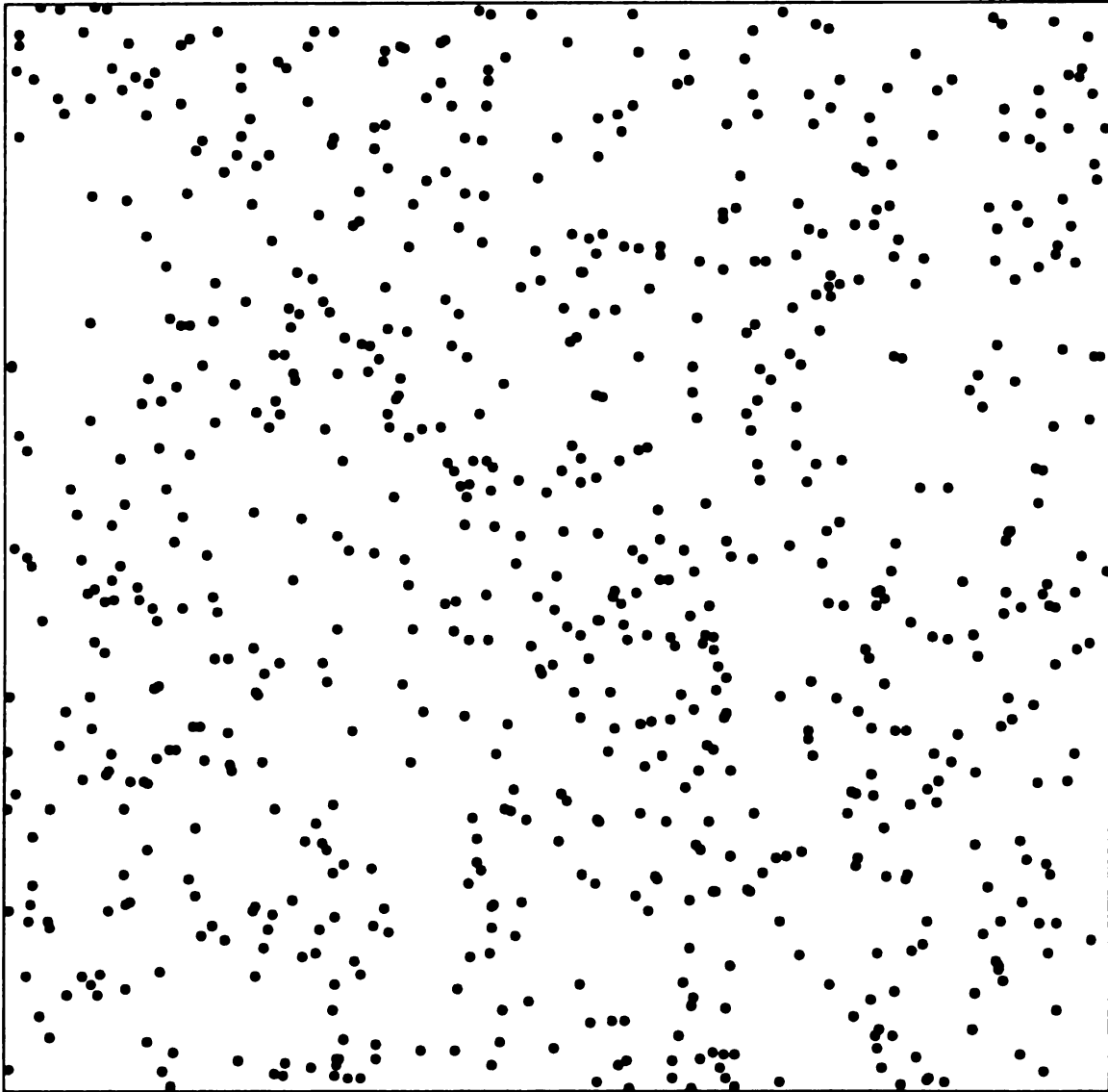


Figure 4-10 Experiment 2, Large Dotted Line Perturbations

4.3 Experiment 3 - Spacing, Longitudinal, Transverse (20)

Figures 4-11 and 4-12 contain all possible line perturbations. The line in Figure 4-11 is immediately obvious while the line in Figure 4-12 is not. Figure 4-12 emphasizes the effect of the background absorbing the structure when the structure to background interdot distance ratio approaches 1.10. Average figure significance measurements plotted for Experiment 3 do not distinguish between the combinations of the longitudinal and transverse variation amounts used. The only distinction made is of the graph type. Also, no points are joined by line segments because the number of points possible at a line spacing of 10 pixels is not equal to the number of points possible at a line spacing of 13 pixels. This is due to the dependency of the longitudinal variation range on the structure spacing and is shown in Figure 3-3. The DT structure detection results of Figure 4-13 agree with those of Figure 4-2 and Figure 4-9. Figure 4-13 gives an indication of how the graphs separate into four groups with some overlap of the neighbors in the graph hierarchy. This overlap is caused by extremes in the perturbation parameter values. For example, for a given line spacing, the DT of a line having plus or minus nine dots longitudinal and plus or minus four dots transverse variation can produce a figure significance value similar to the GG of a line having plus or minus three dots longitudinal and plus or minus two dots transverse variation. At a line spacing of 22 pixels, the most challenging, it is clear that the DT gives the best performance of all the graphs.

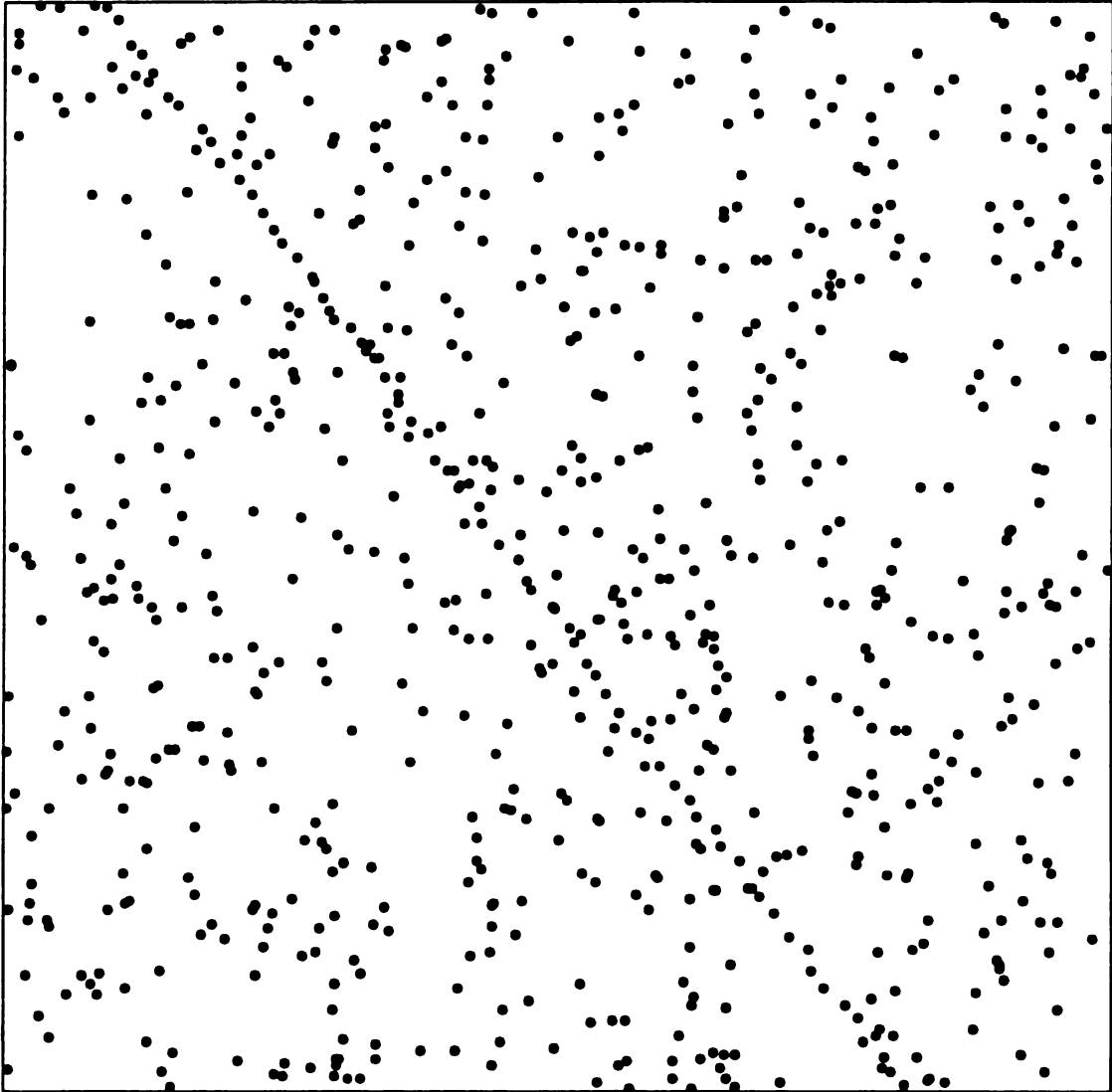


Figure 4-11 Experiment 3, Small Dotted Line Perturbations

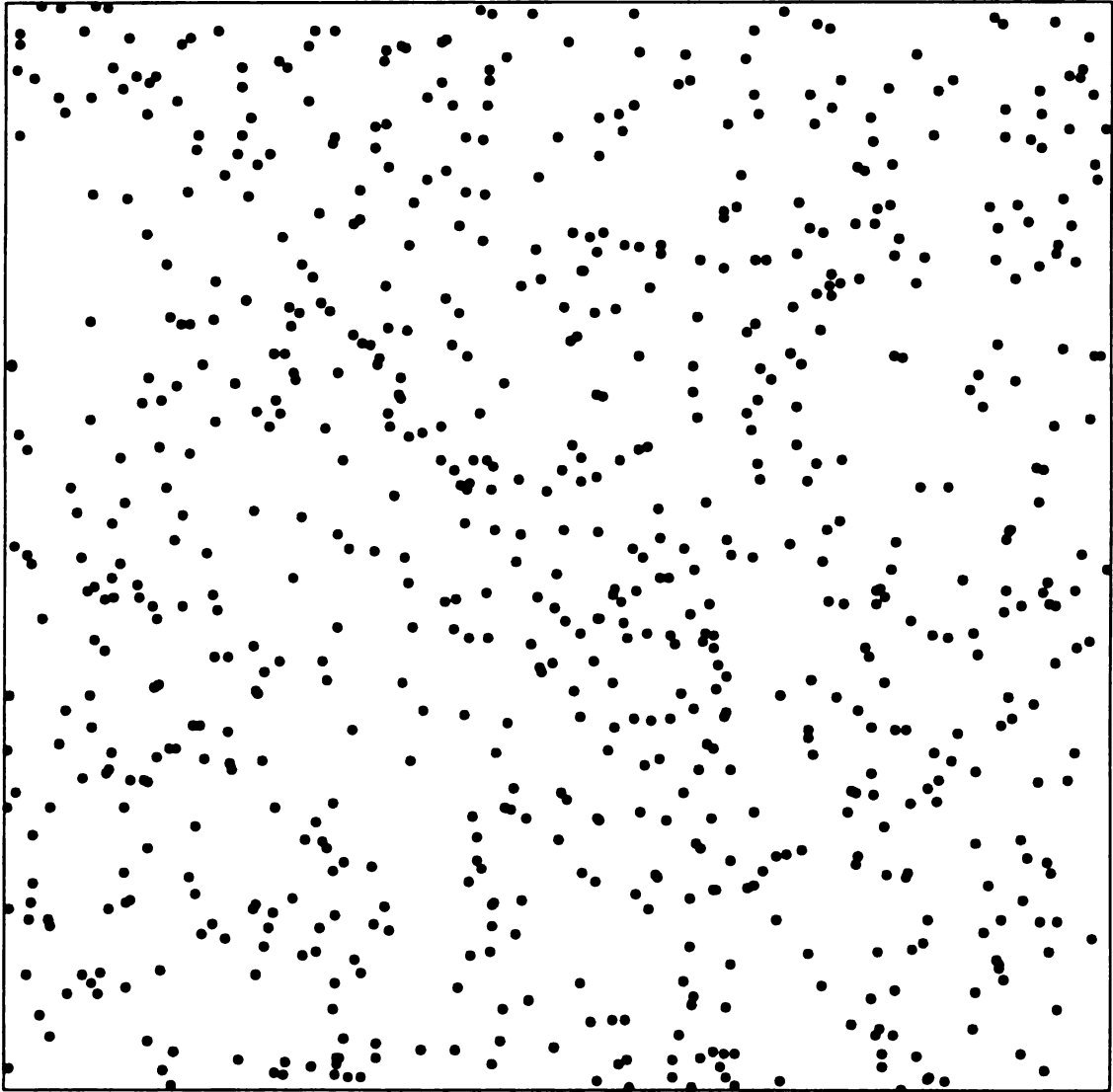
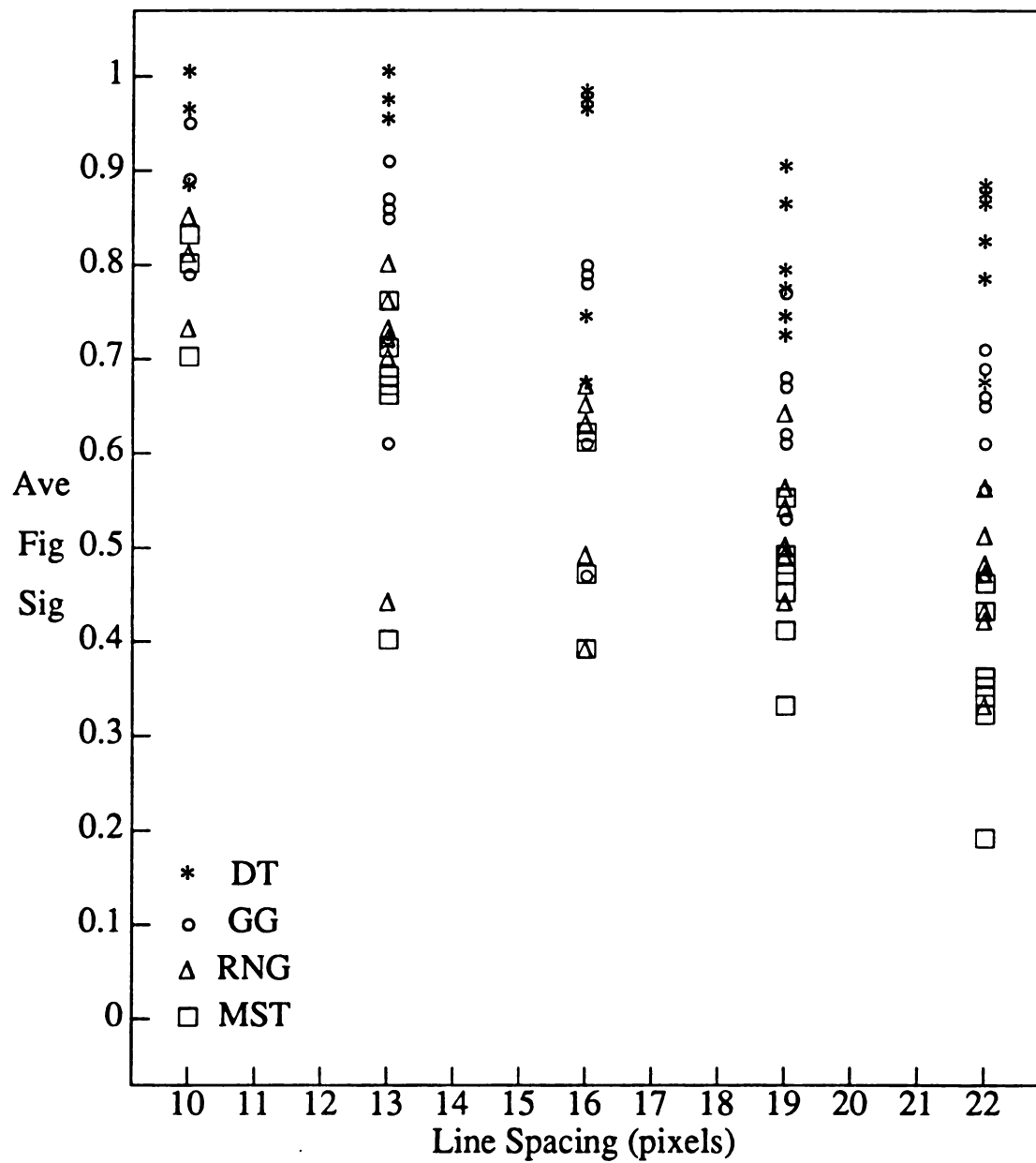


Figure 4-12 Experiment 3, Large Dotted Line Perturbations

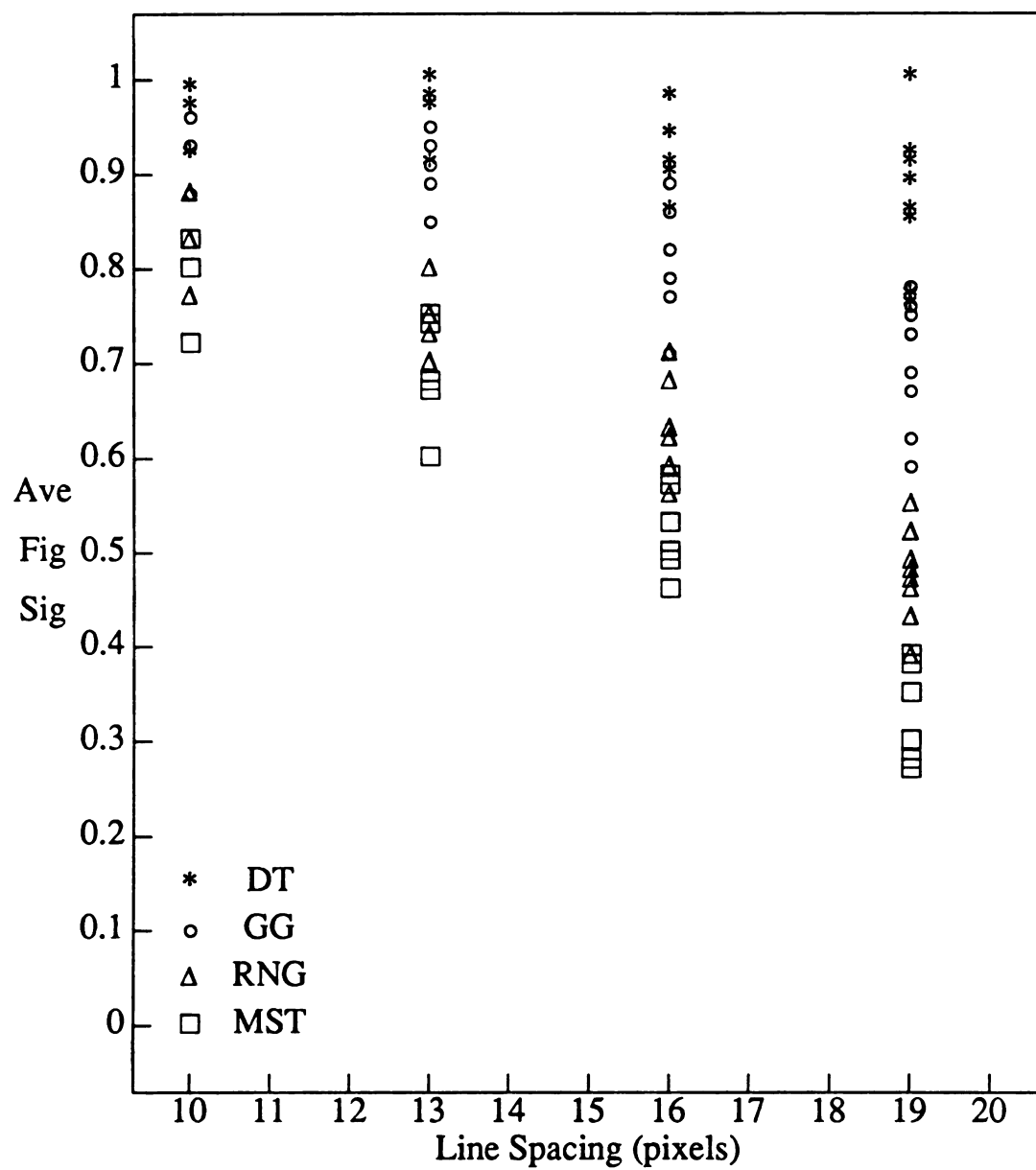


$\pm 3, \pm 6, \pm 9$ Longitudinal and $\pm 2, \pm 3, \pm 4$ Transverse Variations (pixels)

Figure 4-13 Experiment 3, Average Figure Significance Results

4.4 Experiment 4 - Spacing, Longitudinal, Transverse (16)

Experiment 4 is exactly the same as Experiment 3 except for the decrease in the average interdot distance of the background (higher dot density). The superior structure detection capability of the DT exhibited in Experiment 4 supports the findings of Experiment 3 and are plotted in a similar fashion in Figure 4-14. Figures 4-15 and 4-16 show examples of the increased background noise and different degrees of line distortion. Note that in Figure 4-14 at a line spacing of 19 pixels, the four graphs group into a well defined hierarchy.



$\pm 3, \pm 6, \pm 9$ Longitudinal and $\pm 2, \pm 3, \pm 4$ Transverse Variations (pixels)

Figure 4-14 Experiment 4, Average Figure Significance Results

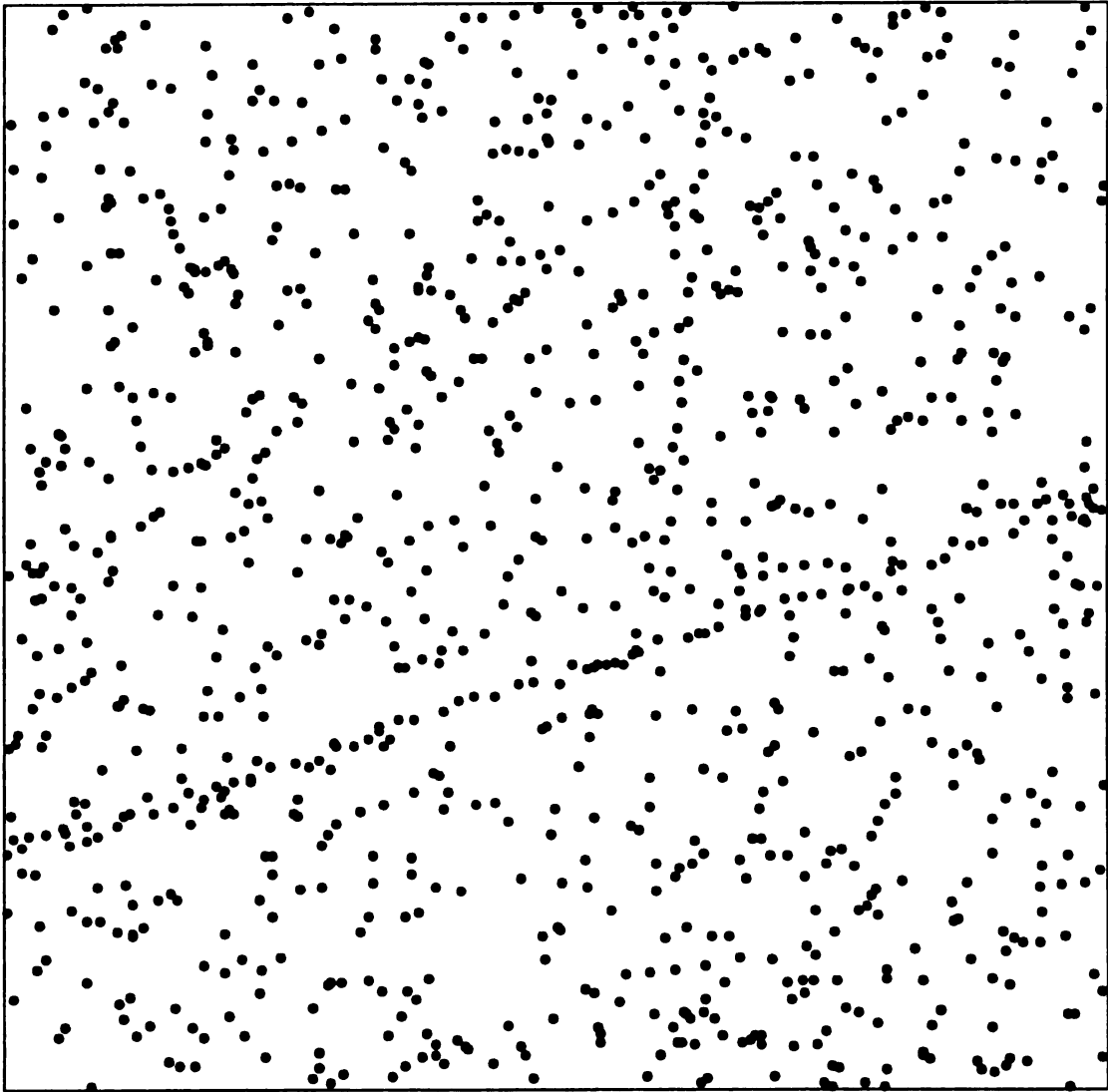


Figure 4-15 Experiment 4, Small Dotted Line Perturbations

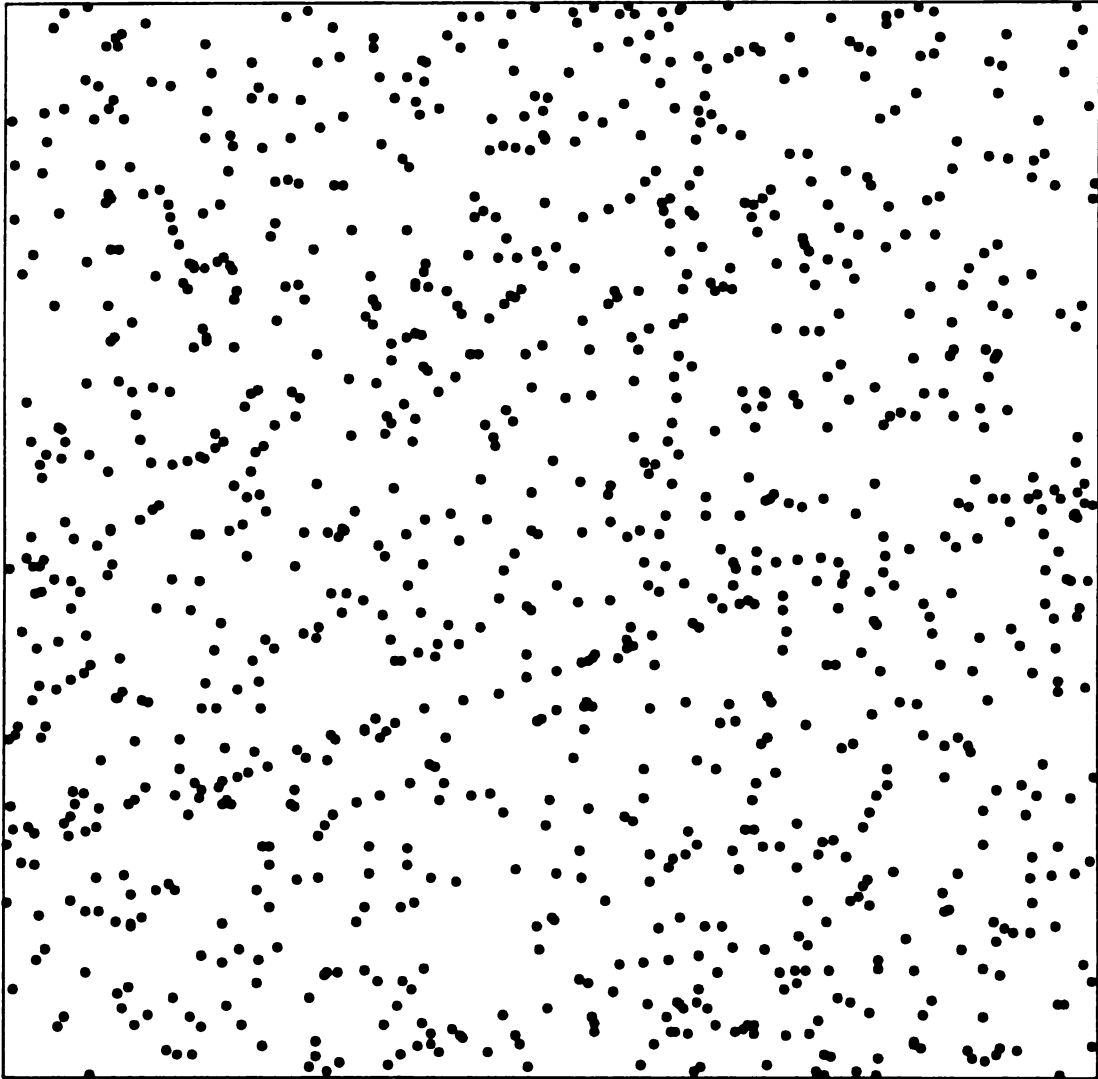


Figure 4-16 Experiment 4, Large Dotted Line Perturbations

4.5 Experiment 5 - Perturbation (20)

In this experiment and the one following, a single dot has been perturbed and the highest order neighbor with altered vertex adjacencies is determined. The average of the highest neighbor orders effected by each dot perturbation is given in Figure 4-17. The trend exhibited by the data shows that the average neighbor order effected by the dot perturbations is larger for the GG, RNG and MST than the DT. The values of the measurement significance Z computed using the average neighbor orders are given in Table 4-1 where an absolute value of Z greater than 1.96 indicates that the difference between the average neighbor orders is significant. Table 4-1 indicates that a significant difference exists between the average neighbor order of the DT and any other graph at dot perturbations greater than or equal to 9 pixels. The only other significant difference between the average neighbor order measurements exists at a dot perturbation of 6 pixels between the DT and the MST. Note the high variances of the MST over the entire dot perturbation range.

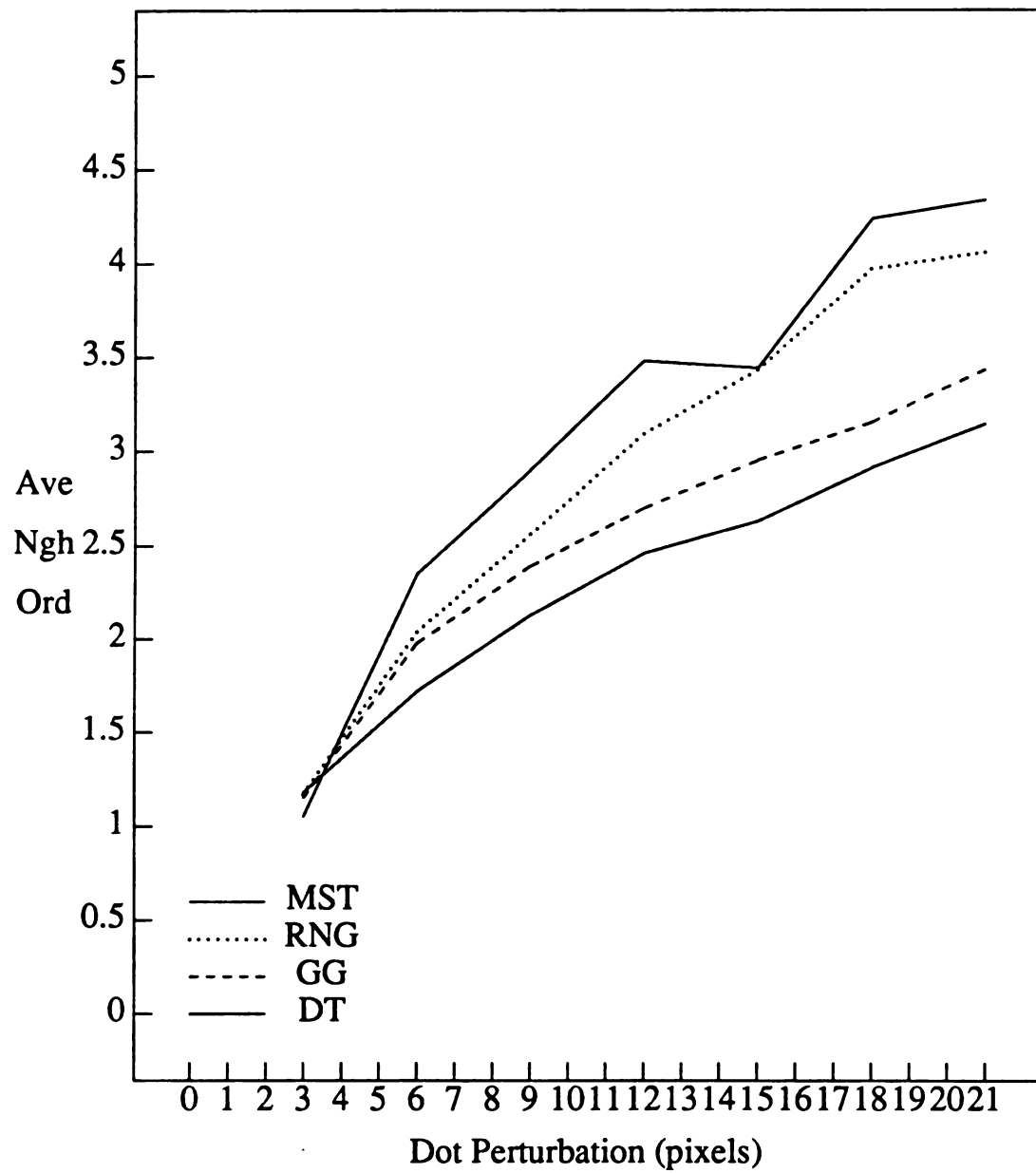


Figure 4-17 Experiment 5, Average Neighbor Order Results

Table 4-1 Experiment 5, Significance of the Average Neighbor Orders. The difference in the average neighbor order measurements (μ) between the DT and any other graph are significant if $|Z| > 1.96$. These values of Z have been marked with an asterisk (*). The variances (σ^2) used in computing Z are also listed.

Dot Perturbation		Graphs			
		DT	GG	RNG	MST
3	μ	1.18	1.15	1.17	1.05
	σ^2	1.33	1.25	2.10	4.13
	Z		-0.19	-0.05	-0.56
6	μ	1.72	1.98	2.04	2.35
	σ^2	1.16	1.04	2.24	7.63
	Z		1.75	1.74	2.13*
9	μ	2.13	2.39	2.56	2.90
	σ^2	0.73	0.72	2.15	7.41
	Z		2.16*	2.53*	2.70*
12	μ	2.46	2.70	3.09	3.48
	σ^2	0.43	0.59	2.08	7.75
	Z		2.38*	3.98*	3.57*
15	μ	2.63	2.95	3.43	3.44
	σ^2	0.45	0.63	2.03	4.99
	Z		3.08*	5.08*	3.47*
18	μ	2.91	3.15	3.97	4.24
	σ^2	0.30	0.69	2.81	7.76
	Z		2.41*	6.01*	4.68*
21	μ	3.14	3.43	4.06	4.34
	σ^2	0.36	0.89	2.46	8.84
	Z		2.60*	5.31*	3.96*

4.6 Experiment 6 - Perturbation (16)

Experiment 6 is a duplicate of Experiment 5 in every way except that the dot density is increased. The high relative stability of the DT's structure indicated by the results of Experiment 6 are in agreement with those of Experiment 5 and are shown in Figure 4-18. The values for the measurement significance Z in Table 4-2 show that the difference between the average neighbor orders is significant for all dot perturbations greater than or equal to 9 pixels. In this experiment however, the significant differences generally occur between the DT and every other graph except the GG. The only significant difference between the average neighbor order of the DT and the GG is at perturbations of 12 and 18 pixels. Again note the high variances of the MST across all dot perturbation amounts.

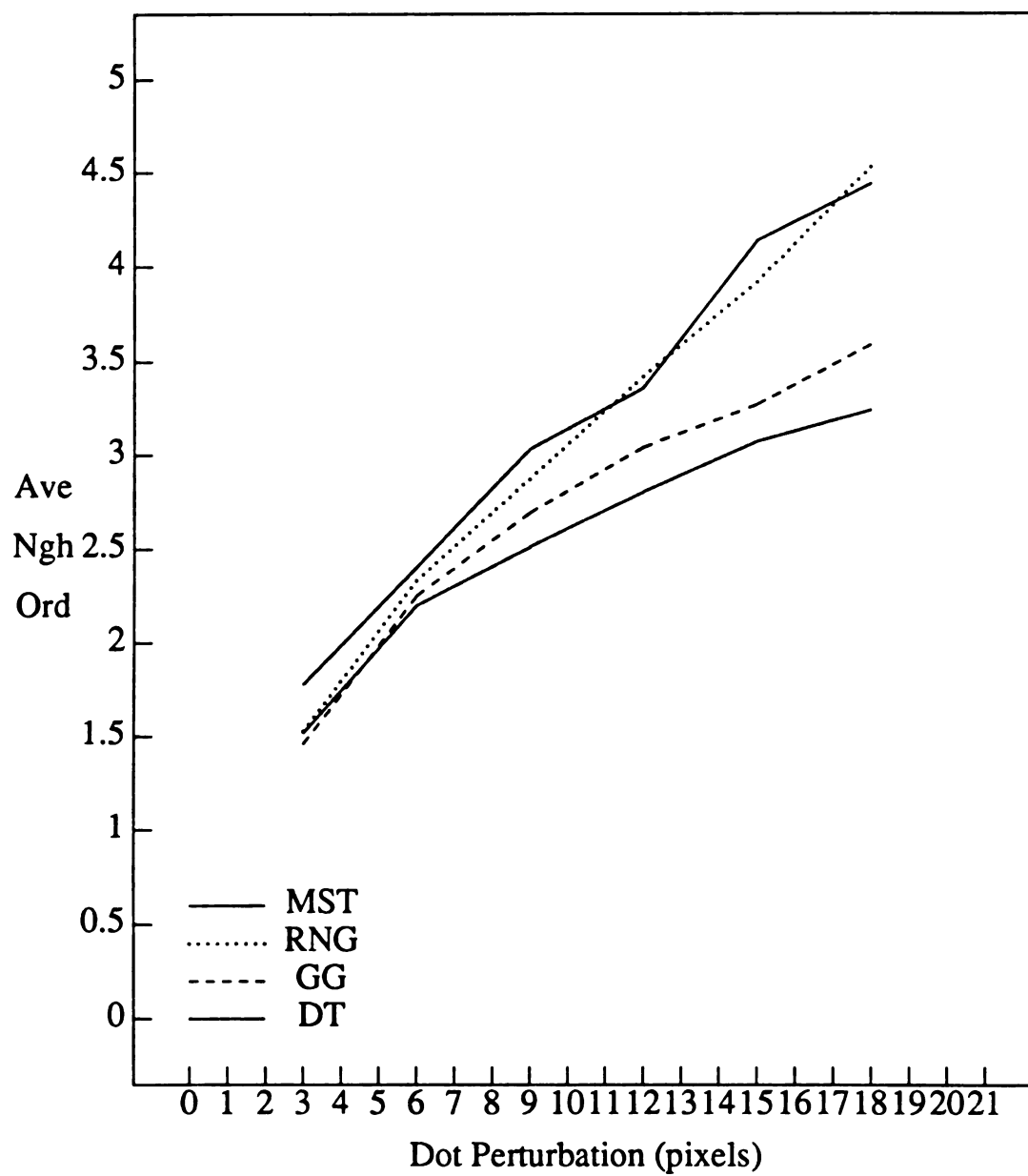


Figure 4-18 Experiment 6, Average Neighbor Order Results

Table 4-2 Experiment 6, Significance of the Average Neighbor Orders. The difference in the average neighbor order measurements (μ) between the DT and any other graph are significant if $|Z| > 1.96$. These values of Z have been marked with an asterisk (*). The variances (σ^2) used in computing Z are also listed.

Dot Perturbation		Graphs			
		DT	GG	RNG	MST
3	μ	1.52	1.46	1.53	1.78
	σ^2	1.09	1.51	2.03	4.95
	Z		-0.37	0.06	1.06
6	μ	2.20	2.25	2.33	2.40
	σ^2	0.52	0.91	2.02	5.70
	Z		0.42	0.82	0.80
9	μ	2.51	2.69	2.87	3.03
	σ^2	0.49	0.79	2.19	5.61
	Z		1.59	2.20*	2.11*
12	μ	2.80	3.04	3.42	3.36
	σ^2	0.46	0.94	2.38	5.03
	Z		2.03*	3.68*	2.39*
15	μ	3.07	3.27	3.92	4.14
	σ^2	0.53	0.94	3.21	7.28
	Z		1.65	4.40*	3.83*
18	μ	3.24	3.59	4.53	4.44
	σ^2	0.44	1.04	4.09	8.11
	Z		2.87*	6.06*	4.10*

Chapter 5

Conclusions

Various graphs have been suggested as tools for detecting structure in random dot patterns. The DT, GG, RNG and MST have been evaluated to determine their relative potential in this area. Additionally, the DT, GG, RNG and MST have been evaluated to determine their relative stability in defining a neighbor relation on image entities. Results have been presented in previous chapters. This chapter draws conclusions from the performance measurements and gives suggestions for future work.

5.1 Summary and Conclusions

The DT, GG, RNG and MST have been examined to determine their relative performance in detecting linear structures implanted in uniformly distributed random dot patterns. Four structure detection experiments have been performed focusing on the detrimental effects that structure dot perturbation has on the graph's ability to retain the neighbor relations among the dots comprising the structure. The types of structure perturbation employed were interdot spacing, longitudinal variation and transverse

variation. The performance of the graphs was quantified by one measure, a figure significance.

The DT, GG, RNG and MST have also been examined to determine their relative structural stability. Two graph stability experiments have been performed focusing on the range of the effect a single dot perturbation has on the graph neighbors. The dot perturbation amount was systematically varied with the direction selected randomly. The stability of the graphs was quantified by the highest order of the neighbors effected by the change.

It is not surprising that all the graphs performed well in the easy cases of the structure detection experiments. All these cases included a dotted line with an interdot spacing much smaller than the average interdot distance of the background. These instances are given in Experiment 1, in Experiment 2 with transverse variations and in Experiments 3 and 4 with a combination of longitudinal and transverse variations. In these situations, the graph neighbor relations of the DT, GG, RNG and MST maintained the connections between the image points that were in close proximity to one another.

Across all structure detection experiments, the general trend is that the performance of each graph degrades when the amount of perturbation increases. This trend holds whether there exists a single type of perturbation or a combination of perturbations. Furthermore, the results exhibit the general tendency of the performance of the DT to degrade slower than the performance of any other graph. Since the neighborhood definition of the DT allows a node to have a greater number of neighbors than any other graph then the DT should suffer the least drop in structure detection

performance. This outcome is most apparent in Figure 4-9 portraying the results of Experiment 2.

Turning to the two graph stability experiments, the pattern that emerges is that when the dot perturbation increases, all the graphs have a higher order neighbor effected. The experimental results indicate that the DT is the best at localizing the effect of single dot perturbations and the MST is the worst. The difference in the sensitivity between the MST and the DT is significant and can be attributed to the global versus local nature of their graph neighborhood definitions.

The major contribution of this thesis lies in the systematic examination of the sensitivity of a family of closest-point graphs. A minor contribution was the development of a measure to quantify the structure detection performance of the DT, GG, RNG and MST. The new results from this study indicate that the DT has the greatest ability to locate dotted linear structures when a relatively high amount of interference is present and is the most structurally stable under single dot perturbations.

5.2 Future Work

The structure detection performance evaluation in this thesis concentrated on the simplest of all dotted structures, the line. The linear case is just one of the many possible structures that need examination. Another form is the circle. The circular case is important because a circle, or one of its relatives, is encountered very frequently in image processing tasks.

Another area of further study would be an investigation concerning the interaction of multiple lines and curves during structure detection. Every image in computer vision is comprised of many straight and curved lines

contributing to the overall shape of each object.

An extension of the graph stability experiments would be to study the effects of multiple dot perturbations on the graph's structure. The graph with the most stable neighbor relation would be very useful in providing information where small distortions are present in multiple images of the same scene.

With the results from this thesis and the areas of future work suggested, the development of a formal algorithm to detect linear structures in arbitrary images using graph neighbor information can be attempted. This algorithm would have to deal with eliminating noise lines whose points are all graph neighbors. One possible solution would be to calculate the figure significance and multiply it by a measure that would be able to distinguish if the dots of the candidate structure are from the same population as the surrounding environment. If the dots of the structure are of the same population as the background, then the measurement should be low and when multiplied by the figure significance would produce a low overall value thereby eliminating the noise line from further consideration. Otherwise, the measurement should be high giving a high overall rank after multiplication and labeling the line as a valid structure.

The DT may not be practical for all situations where linear structure needs to be located. If the magnitude of the variations are known to be limited to the range where the MST does well then the MST is the better choice. However, if nothing is known about the linear structure perturbations present in an image or if the range of the perturbations is unrestricted then the DT is a worthy candidate for providing reliable graph neighbor information in linear structure detection tasks.

Bibliography

- [AHU 82] Ahuja N., "Dot Pattern Processing using Voronoi Neighborhoods", *IEEE PAMI*, V4, 1982, pp. 336-343.
- [BAL 81] Ballard D. H., "Generalizing the Hough Transform to Detect Arbitrary Shapes", *Pattern Recognition*, V13, 1981, pp. 111-122.
- [BOX 58] Box G. E. P., Muller M. E., "A Note on Generation of Normal Deviates", *Annals of Mathematical Statistics*, V28, 1958, pp. 610-611.
- [BRO 83] Brown C. M., "Inherent Bias and Noise in the Hough Transform", *IEEE PAMI*, V5, 1983, pp. 493-505.
- [CAS 87] Casasent D., Krishnapuram R., "Curved Object Location by Hough Transformations and Inversions", *Pattern Recognition*, V20, 1987, pp. 181-188.
- [DUD 72] Duda R. O., Hart P. E., "Use of the Hough Transformation to Detect Lines and Curves in Pictures", *CACM*, V15, 1972, pp. 11-15.
- [FAI 83] Fairfield J., "Segmenting Dot Patterns by Voronoi Diagram Concavity", *IEEE PAMI*, V5, 1983, pp. 104-110.

- [GEB 67] Gebhardt F., "Generating Pseudo-Random Numbers by Shuffling a Fibonacci Sequence", *Mathematics of Computation*, V21, 1967, pp. 708-709.
- [GRE 78] Green P. J., Sibson R., "Computing Dirichlet Tessellations in the Plane", *Computer Journal*, V21, 1978, pp. 168-173.
- [HOU 62] Hough P. V. C., "Method and Means for Recognizing Complex Patterns", *U. S. Patent 3069654*, 1962.
- [ILL 87] Illingworth J., Kittler J., "The Adaptive Hough Transform", *IEEE PAMI*, V9, 1987, pp. 690-698.
- [JAR 73] Jarvis R. A., Patrick E. A., "Clustering using a Similarity Measure Based on Shared Near Neighbors", *IEEE C*, V22, 1973, pp. 1025-1034.
- [KOF 35] Koffka K., *Principles of Gestalt Psychology*, Harcourt Brace and Jovanovich, 1935.
- [KRU 56] Kruskal J. B. Jr., "On the Shortest Spanning Subtree of a Graph and the Traveling Salesman Problem", *Proceedings of the American Mathematical Society*, V7, 1956, pp. 48-50.
- [MAI 86] Maitre H., "Contribution to the Prediction of Performances of the Hough Transform", *IEEE PAMI*, V8, 1986, pp. 669-674.
- [MAR 62] Marsaglia G., "Random Variables and Computers", *Transactions of the Third Prague Conference on Information Theory, Statistical Decision Functions, Random Processes*, Czechoslovak Academy of Sciences, 1962, pp. 499-510.
- [MAT 80] Matula D. W., Sokal R. R., "Properties of Gabriel Graphs Relevant to Geographic Variation Research and the Clustering of Points in the Plain", *Geographical Analysis*, V12, 1980, pp. 205-222.
- [PRE 85] Preparata F. P., Shamos M. I., *Computational Geometry, An Introduction*, Springer-Verlag, 1985.

- [PRI 57] Prim R. C., "Shortest Connection Networks and Some Generalizations", *Bell Systems Technical Journal*, V36, 1957, pp. 1389-1401.
- [ROS 73] Rosenberg B., Langridge D. J., "A Computational View of Perception", *Perception*, V2, 1973, pp. 415-424.
- [SHA 75] Shamos M. I., Hoey D., "Closest-Point Problems", *Proceedings of the Annual Symposium on the Foundations of Computer Science*, 1975, pp. 131-162.
- [SHA 79] Shapiro S. D., Iannino A., "Geometric Constructions for Predicting Hough Transform Performance", *IEEE PAMI*, V1, 1979, pp. 310-317.
- [SKL 78] Sklansky J., "On the Hough Technique for Curve Detection", *IEEE C*, V27, 1978, pp. 923-926.
- [TOU 80A] Toussaint G. T., "Pattern Recognition and Geometrical Complexity", *Proceedings of the IEEE International Conference on Pattern Recognition*, 1980, pp. 1324-1347.
- [TOU 80B] Toussaint G. T., "The Relative Neighbourhood Graph of a Finite Planar Set", *Pattern Recognition*, V12, 1980, pp. 261-268.
- [TOU 87] Toussaint G. T., "Computational Geometry: Recent Results Relevant to Pattern Recognition", *NATO Advanced Study Institute on Pattern Recognition Theory and Applications*, V30, 1987, pp. 295-305.
- [TUC 86] Tuceryan M., "Extraction of Perceptual Structure in Dot Patterns", PhD. Thesis, University of Illinois at Urbana-Champaign, 1986.
- [URQ 82] Urquhart R., "Graph Theoretical Clustering Based on Limited Neighbourhood Sets", *Pattern Recognition*, V15, 1982, pp. 173-187.
- [VAN 81] van Veen T. M., Groen F. C. A., "Discretization Errors in the Hough Transform", *Pattern Recognition*, V14, 1981, pp. 137-145.

- [VIS 87] Vistnes R. "Detecting Dotted Lines and Curves in Random-Dot Patterns", *Proceedings of the DARPA Image Understanding Workshop*, V2, 1987, pp. 849-861.
- [VOR 08] Voronoi M. G., "Nouvelles Applications des Parametres Continus a la Theorie des Formes Quadratiques. Deuxieme Memoire. Recherches sur les Paralleloedres Primitifs.", *Journal fur die Reine und Angewandte Mathematik*, V134, 1908, pp. 198-287.
- [WAR 62] Warshall S., "A Theorem on Boolean Matrices", *JACM*, V9, 1962, pp. 11-12.
- [WER 38] Wertheimer M., *Laws of Organization in Perceptual Forms from a Source Book of Gestalt Psychology*, Harcourt Brace and Jovanovich, 1938.
- [ZAH 71] Zahn C. T., "Graph-Theoretical Methods for Detecting and Describing Gestalt Clusters", *IEEE C*, V20, 1971, pp. 68-86.